FACULTY OF SCIENCES

WALRUS FOSSILS FROM *HET SCHEUR* OFF THE BELGIAN COAST: REMAINS OF A LATE PLEISTOCENE COLONY?

Hendrik Plas
Student number: 01510344

Promotor: Prof. dr. Stephen Louwye
Copromotor: Dr. Leonard Dewaele

Jury: Dr. Olivier Lambert, Prof. dr. Dominique Adriaens

Master's dissertation submitted in partial fulfilment of the requirements for the degree of master in geology

Academic year: 2020-2021

GHENT UNIVERSITY

KU LEUVEN

ACKNOWLEDGEMENTS

I would like to thank my promotor prof. dr. Stephen Louwye from Ghent university for his help and the opportunity he gave me to work on this subject. I thank my copromotor dr. Leonard Dewaele from Liège university for his counsel and for leading me in the right direction for completing this master's dissertation and providing answers to my questions. I'm also grateful to dr. Olivier Lambert from the Royal Belgian Institute of Natural Sciences (IRSNB) for his help. I thank Bram Langeveld, Dick Mol and Klaas Post from the Museum of Natural History of Rotterdam (NMR), the Flanders Marine Institute (VLIZ) and the crew of the VLIZ's RV Simon Stevin who collaborated for the collection of most of the recent walrus specimens. I thank dr. Pascal Hablützel and dr. Tine Missiaen from the VLIZ, for facilitating the transfer of the trawled walrus fossils to the paleontological collection of the Royal Belgian Institute of Natural Sciences. I also thank curators of the IRSNB paleontological collection, dr. Annelise Folie and Olivier Pauwels, for their help.

TABLE OF CONTENTS

1 INTRODUCTION

The Southern North Sea Basin is known as an area that is very rich in Pleistocene fossils (De Clercq, 2018; Missiaen et al., 2019; Post et al., 2017; Vermeersch et al., 2015). Over the last few years, fossil remains of Late Pleistocene megafauna such as elephants, aurochs and giant deer have been collected from *Het Scheur*, a navigation channel northeast off the Zeebrugge harbour on the Belgian Coast. These specimens have been collected by beam trawling of the seafloor by researchers of the Flanders marine institute (VLIZ) and the Natural History Museum Rotterdam (NMR) during several campaigns between 2015 and 2018 (Langeveld, 2018; Missiaen et al., 2019; Post et al., 2017). Among the fossil finds, was especially a large number of 42 bone fragments from juvenile and adult walruses (*Odobenus rosmarus*). Jan Seys, spokesperson of the VLIZ indicated in an interview to with the VRT that more than 300 walrus fossils have been collected in the area over the past 20 years belonging to at least 50-100 individuals (VRT NWS, 2018). Because the fossils show no or little signs of abrasion, therefore indicating almost no secondary transport, it has been suggested that they were found *in situ* as the accumulation of bones from an on-shore colony, which would make this the southernmost known Pleistocene walrus colony in the world (Langeveld, 2018; Seys, 2017). Radiocarbon dating of some of the bones yields ambiguous ages between 44-50 ka as this is around the limit of the radiocarbon dating method. However, recent paleogeographic reconstructions suggest that the walrus bone material stems from the Late Eemian to Early Glacial, as the Southern Nord Sea Basin was mostly above sea level during the Last Glacial (De Clercq, 2018; Missiaen et al., 2019).

Today, walruses live in colonies of separate sexes, which means there are either colonies with only males or with females and juvenile walruses, which only gather together during the mating season (Born et al., 1995; Fay, 1982; Lydersen, 2018). The aim of this study is to determine the sexual makeup of the fossil record and see if there is a predominance of either male or female and juvenile walruses. This will be done by examining the different walrus bones that were collected and try to determine the sex of each specimen as far as possible. An approximation of the age and of the different fossils and the age distribution is also carried out by assessing at the skeletal maturity of the bones to distinguish the younger from the older animals. By analysing the ratio males/females & juveniles, I try to elucidate the sexual and ontogenetic makeup of this fossil record in order to assess the paleontological history of the Pleistocene walruses at *Het Scheur*.

2 LIFE AND HISTORY OF THE WALRUS (*ODOBENUS ROSMARUS)*

2.1 Taxonomic classification

The walrus, *Odobenus rosmarus,* is the only extant member of the Odobenidae family, which forms together with the Otariidae (fur seals and sea lions) and Phocidae (true or earless seals) and the extinct Desmatophocidae the carnivorian suborder of the Pinnipedia (fig. 1). The walrus distinguished from other extant pinnipeds by the enlarged upper canines. The scientific name *Odobenus rosmarus,* meaning tooth-walking sea horse, refers to the fact that they pull themselves up onto the ice using their tusks (Lydersen, 2018).

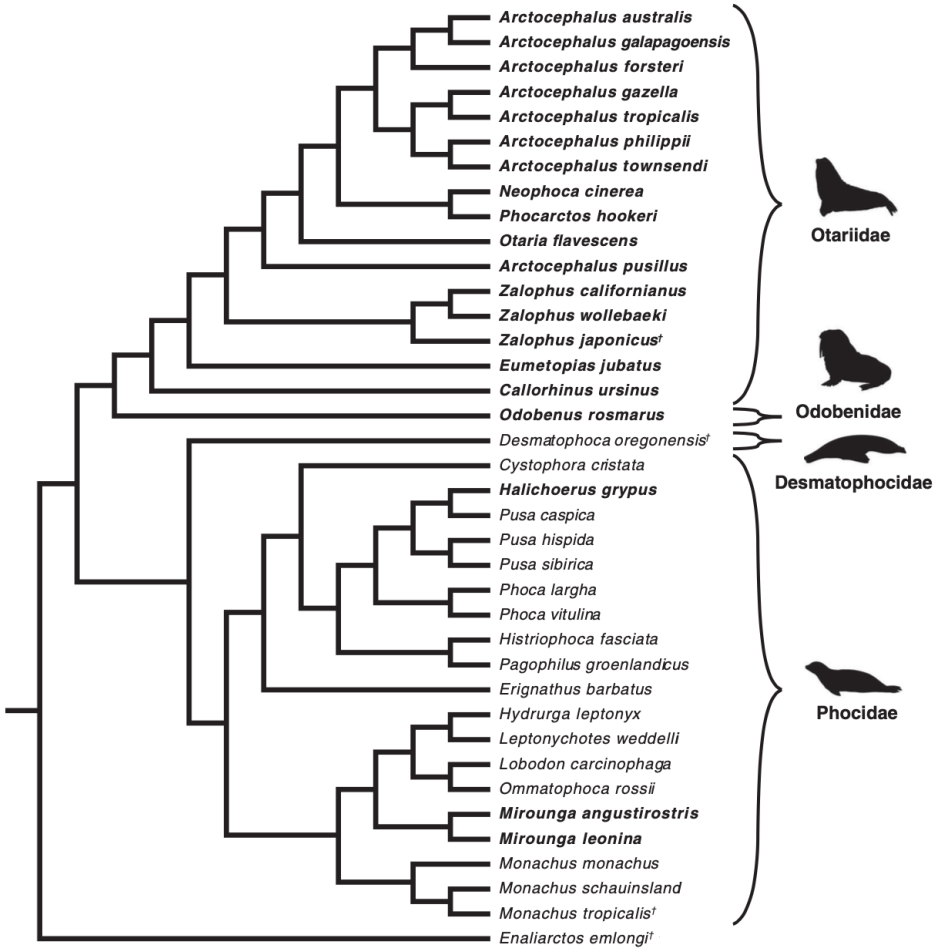

Figure 1: *Phylogeny of the pinnipeds. Modified after Cullen et al. (2014).*

Odobenids are a monophyletic group which is defined by Boessenecker and Churchill (2013) based on the presence of a large, thick-margined, dorsoventrally elliptical anterior narial opening; a large epitympanic recess; a thick, broad pterygoid strut; bony tentorium appressed to petrosal and a triple-rooted M^1. Although the tusks are the most characteristic features of the modern walrus, they are absent in many extinct walrus species form the Odobenid family (Berta et al., 2018; Deméré and Berta, 1994;

Repenning and Tedford, 1977). There are two recognised extant subspecies of *Odobenus rosmarus*: the Pacific walrus, *Odobenus rosmarus divergens* (Illiger, 1815) and the Atlantic walrus *Odobenus rosmarus rosmarus* (Linnaeus, 1758). The distinction between both subspecies is based on morphological characteristics and mitochondrial DNA (Kastelein, 2002; Lydersen, 2018). A detailed description of the differences has been given by Allen, (1880). *O. r. divergens* is on average larger in size and heavier than *O. r. rosmarus* (an average of 320 cm total body length and 1210 kg body weight for *O. r. divergens* compared to 314 cm and 1114 kg for *O. r. rosmarus* for adult males) (Fay, 1982; Knutsen and Born, 1994), but the most prominent difference lies in the facial outline. The tusks of *O. r. divergens* are longer and thinner, generally more convergent and have a greater inward curvature. The facial region of *O. r. divergens* is broader and its occipital region is smaller than that of *O. r. rosmarus*. As their names indicate, the Atlantic walrus lives in the northern Atlantic and the Pacific walrus the northern Pacific. The divergence between both subspecies was calculated by Cronin et al. (1994) between 500 and 785 ka, probably as a result of the splitting of the population in different groups by glaciations (Davies, 1958). A possibly third subspecies, the Laptev walrus, *Odobenus rosmarus laptevi* (Chapskii, 1940), is now, based on recent DNA analysis, assumed to be the westernmost stock of the Pacific walrus (Lindqvist et al., 2009).

2.2 Evolution and fossil record

The first odobenids appeared in the early Miocene (16-18 Ma) (Berta, 2018). There are three major groups of odobenids that have been identified: the stem “imagotariines”, the dustignathines and the odobenines (fig. 2). The fossil odobenid record is with 21 known species in 17 genera, the fossil record of odobenids is more diverse than today’s diversity, with only one extant member (*Odobenus rosmarus*) (Berta et al., 2018).

Odobenids have their first appearance in the North Pacific with the small-bodied “imagotariines” in the early Miocene (16-18 Ma), with *Prototaria* (Japan) and *Proneotherium* (Oregon, US) (fig. 2). “Imagotariines” is a paraphyletic group which includes stem walruses ancestral to dustignathines and odobenines, and thus no official taxonomic group (Boessenecker and Churchill, 2013; Deméré and Berta, 1994). These stem walruses have unenlarged canines and narrow, multiple rooted premolars with a trend towards molarization. The middle Miocene fossil record shows species with a more diverse body sizes such as *Neotherium mirum* and *Pelagiarctos thomasi* (Barnes, 1988; Berta et al., 2018;

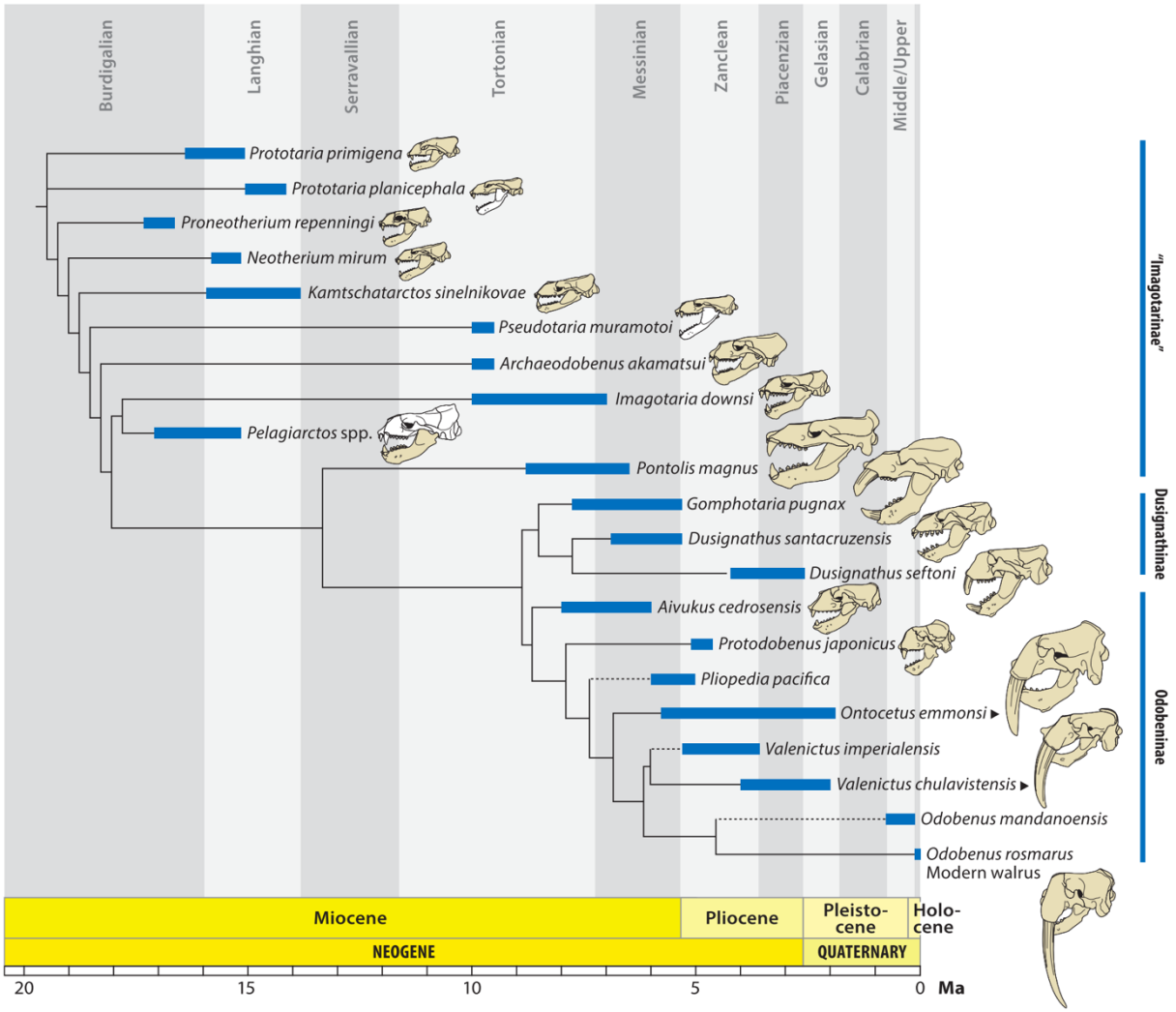

***Figure 2**: Time-calibrated phylogeny of the fossil record of odobenids with an illustration of the changes in skull morphology (Berta et al., 2018).*

Kohno et al., 1995). Unlike the true walruses from the odobenine subfamily, “imagotariines” are not known to be adapted for a specialized mollusc diet, but instead appear to retained a primitive piscivorous diet, similar as sea lions and fur seals from the otariid subfamily (Deméré and Berta, 2001; Kohno, 1994; Kohno et al., 1995).

During the Miocene, dustignathines and odobenines diverged from the “imagotariines” and remained endemic to the eastern North Pacific until the early Pliocene (Berta et al., 2018; Kohno et al., 1995). Dustignathines are characterized by the development of enlarged, procumbent tusk-like upper and lower canines and large skull. Examples are *Gomphotaria pugnax* and *Dusignathus santacruzensis* from the late Miocene and the Pliocene *Dusignathus seftoni* (fig. 2) (Barnes and Raschke, 1991; Deméré, 1994). Their unusually stocky forelimb bones might suggest otariid-like forelimb-dominated swimming (Berta et al., 2018). Tusk wear and tooth breakage of *Gomphotaria* might imply that shells were broken instead

of being sucked out (Berta, 2018). *Pontolis magnus* from the upper Miocene of Oregon is the largest odobenid with a skull of 60 cm long and a body length of 6 m (Berta et al., 2018; Boessenecker and Churchill, 2013; Deméré and Berta, 1994; Kohno, 2006).

Odobenine fossils are known from the North Atlantic and North Pacific. The late Miocene tuskless *Aivukus cedrosensis* (fig. 3) from the subtropical Baja California is the earliest known odobenine (Repenning and Tedford, 1977). The tribe Odobenini assembles the long-tusked walruses with inflated maxillae, enlarged tusks, highly vaulted palates, reduced sagittal and nuchal crests, and have a trend towards postcanine tooth reduction (Berta et al., 2018). The earliest clear Odobenini appear in the early Pliocene with the small tuskless *Protodobenus* (fig. 3) from Japan (Horikawa, 1994) and *Pliopedia*, which is not completely known (Berta et al., 2018; Kellogg, 1922; Repenning and Tedford, 1977).

Fossils of the Pliocene walrus *Ontocetus emmonsi* (fig. 2) have been classified under different senior synonyms in the past such as *Prorosmarus alleni,Trichechodon huxleyi*, *Alachtherium antverpiensis or Alachtherium crestii* (Berta et al., 2018; King, 1964; Post, 2004), but its complicated taxonomic history has recently been clarified by Kohno and Ray (2008) who showed that these are all belonging to the same species. *Ontocentus* was 15 % larger than the extant Odobenus and was characterized by a rectangular occipital field; more procumbent, shorter and more curved tusks; retention of I^2 and M^1 and an unfused mandibular symphysis (Berta et al., 2018; Kohno and Ray, 2008). The habitat of *Ontocetus* is known to have extended in the North Atlantic from the shores from Florida to New Jersey in the western North Atlantic and from the North Sea down to Morocco in the eastern North Atlantic. Other specimens of *Ontocetus* from Japan implies a dispersal via the Artic during the Pliocene (Kohno et al., 1995; Tomida, 1989). *Odobenus* and its sister taxon *Valenictus* from the Pliocene California share a fused mandibular symphysis and extensive osteosclerosis of the postcranial skeleton (Deméré, 1994). The species *Valenictus chulavistensis* (fig. 2) is different from all other odobenids by the loss of all teeth except canines (Deméré, 1994; Mitchell, 1961), most likely an adaptation to mollusc suction feeding (Deméré, 1994; Fay, 1982).

The earliest *Odobenus* record is from Japan, with a latest Pliocene-early Pleistocene age. Fossils from the Middle and Late Pleistocene are found as far south as San Francisco (California, US) in the Northeast Pacific (Gingras et al., 2007; Harington, 1984) and South Carolina and France in the North Atlantic (Kardas, 1965; Sanders, 2002), suggesting a wider environmental tolerance than today (Kohno et al., 1995). Because the Pliocene *Odobenus* fossils from Japan predate the North Atlantic fossils, a

North Pacific origin is suggested for the taxon, followed by a dispersion to the North Atlantic via the Central American Seaway or the Arctic Ocean during the latest Pliocene, when glacial conditions did not yet exist in the Arctic region (Berta et al., 2018; Kohno et al., 1995).

2.3 Present distribution and abundance

The present walrus, *Odobenus rosmarus*, has an intermittent Arctic circumpolar distribution, where they live in shallow coastal areas (fig. 3). Walruses generally do not live in areas with a water depth of more than 80 to 100 m, possibly because they cannot of dive to greater depths or because they are not able to feed efficiently enough (Fay, 1982; King, 1964). Snow-covered ice floes are preferred as haul-out locations rather than on land, probably because there is less disturbance and because of the proximity of food, as the ice transports them to new feeding grounds while they rest (Fay, 1982).

Odobenus rosmarus divergens is generally found from the Bering Sea up to Bristol Bay (Alaska, US) in the south and the central range of the Chukchi Sea to the Beaufort Sea in the East and the Laptev Sea in the West (Fay, 1982; Kastelein, 2002; King, 1964; Lydersen, 2018). *O. r. divergens* has the largest abundance with an estimation of 135,000 animals (Laidre et al., 2015; Lydersen, 2018).

The *Odobenus rosmarus rosmarus* occurs in the North Atlantic, in the west in a large part of the Eastern Canadian Archipelago and the west coast of Greenland and in the west on the northeast coast of Greenland, the Svalbard and Franz Josef archipelagos and in the Southern Barents Sea Region, mainly in the Kara and Pechora Seas. Historically, *O. r. rosmarus* was also present south to the Gulf of St Lawrence (Canada), but due to extensive hunting they disappeared in the southern regions of their distribution (Born et al., 1995). The abundance of the *O. r. rosmarus* population is much smaller than the *O. r. divergens* with approximately 30,000 animals (Laidre et al., 2015; Lydersen, 2018).

Walruses are migratory. *O. r. divergens* spends the winter in the Bering Sea and migrate northward in summer to the Chukchi Sea, following the retreat of the edges of the ice pack. They move back to the south in October when the ice advances again (Fay, 1982; King, 1964). Similar migratory behaviour has been recorded of *O. r. rosmarus* from the west coast of Greenland, but not every year (Fay, 1982; King, 1964). Little is known about migrations of the *O. r. rosmarus* in Europe, but it is assumed that they stay closer to the coast in winter (Born et al., 1995; King, 1964). Females also tend to be more migratory than males (Fay, 1982).

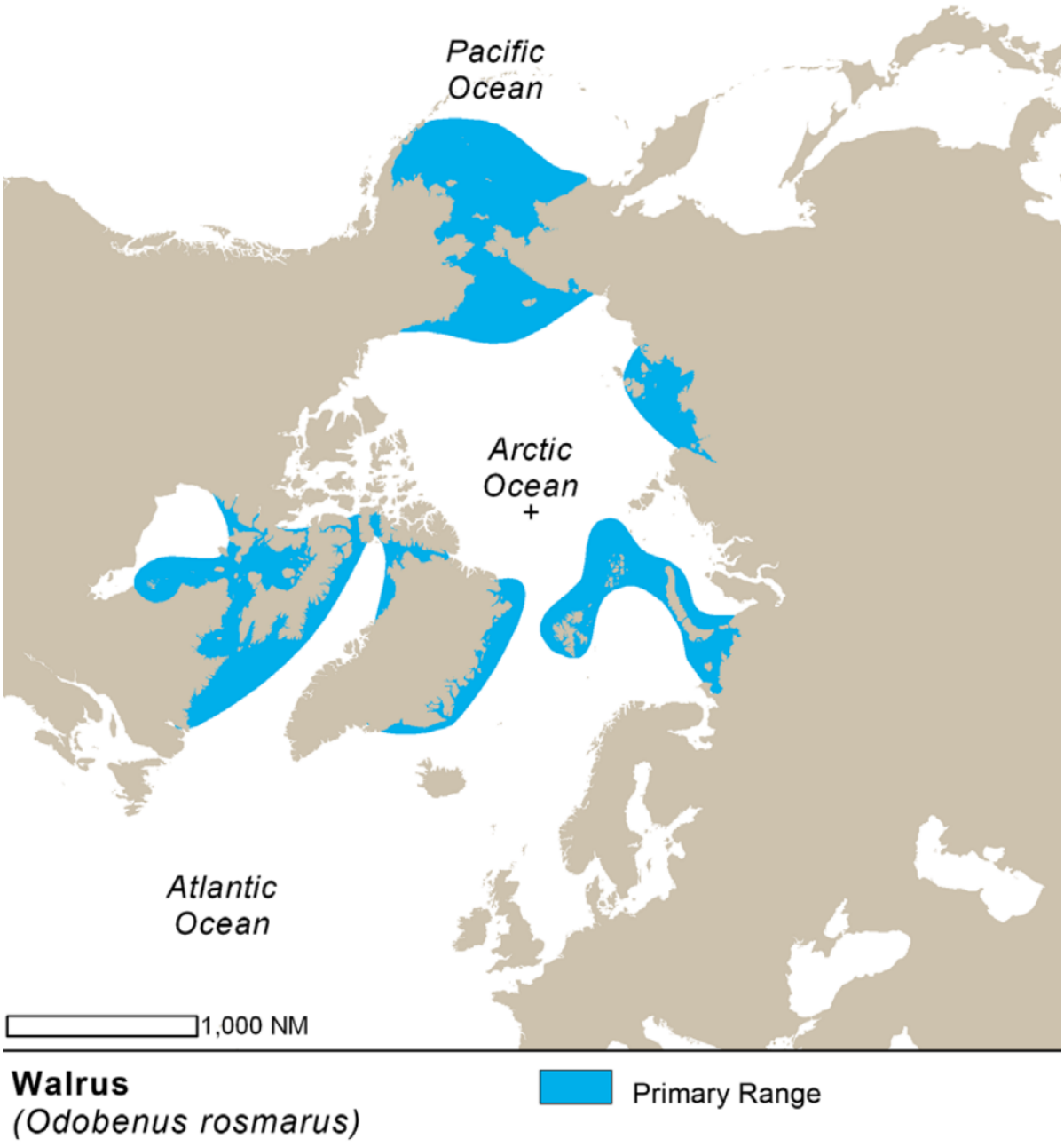

***Figure 3**: Global distribution of the present walrus populations (Lydersen, 2018).*

2.4 External Characteristics

The walrus has a yellowish-brown skin colour, which can sometimes look whiter after diving or pink when they are warm, caused by the change in blood supply to their skin (Kastelein, 2002). The skin can be very thick, about 2-4 cm, heavily wrinkled and covered with tubercles, especially by males. The thickest skin (4 cm) is located in the neck and in the area above the whiskers. The skin in the neck is thicker in adult males than in females and is covered with tubercles, which are 1 cm thicker than the

surrounding skin and serves as protection against attacks by other males (Kastelein, 2002; Lydersen, 2018).

Compared to the other pinnipeds, the eyes, positioned high on the head, are small relative to their body size and can be retracted or protruded. Unlike otariids, but similar to phocids, they have no external ear flaps and the earholes are protected by a fold of skin. The most distinctive characteristics of the walrus are the enlarged upper canines (Kastelein, 2002; Lydersen, 2018). To accommodate their large tusks, the snout is much broader and higher compared to the other extant pinnipeds. They appear in both male and female animals and can grow up to 1 m long and weigh 5 kg. Tusks continue to grow throughout their life but are abraded and frequently broken off due to percussive contacts with hard objects. Their main function is as socially display organs and weapons for male-on-male fighting during the mating season (Fay, 1982; Miller, 1975). Odobenids are able to walk on all four limbs on land by bringing their hind flippers under their bodies, similar like otariids. This is in contrast to phocids, where their body weighs too heavy to be supported by their flippers cannot on land. Because of their massive size, the movement of walruses on land appears clumsier than otariids and adults cannot lift their belly off the substrate (Fay, 1982; Kastelein, 2002; Lydersen, 2018). Locomotion in water, on the other hand, is easier, where the hind limbs are used for propulsion and the front limbs for steering, which is similar as phocids. This is in contrast to otariids, where swimming is powered by their front flippers and the hind limbs are used for turning and stopping (Fay, 1982; Hocking et al., 2021; Kastelein, 2002; Lydersen, 2018).

Adult males, i.e. bulls, can reach a length of 3-3.5 m and weigh around 1200-1500 kg. Adult females, i.e. cows, are smaller with a length of 2.5 m and a weight of about 600-700 kg. Differences can occur between the different populations (Born et al., 1995; Knutsen and Born, 1994). The calves are born with a weight of approximately 60 kg and are about 1.3 m long. The average longevity of walruses lies between 30 and 40 years old. The annual mortality of males is slightly higher than females in the first 6-8 years and much higher (about 13 % for males) thereafter (Born et al., 1995; Fay, 1982; Kastelein, 2002; King, 1964; Lydersen, 2018). The juvenile mortality is low compared to other pinnipeds, due to the long period of parental care (Fay, 1982).

2.5 Sexual dimorphism

Sexual dimorphism is considerable in walruses, with adult males being approximately 10-15 % times longer than adult females and up to twice as heavy (fig. 4) (Garlich-Miller and Stewart, 1998; Knutsen and Born, 1994). This sexual size dimorphism can be attributed to their polygynous mating system (Cullen et al., 2014). Newborn calves do not show sexual dimorphism yet, but it becomes more pronounced in subadult and adult animals. The size difference between both sexes rises from a different length of the growth period, which lasts until the age of 9 for females and 14 for males (Garlich-Miller and Stewart, 1998). The most distinctive differences in morphology can be seen in the skulls. The tusks of the males are larger and thicker than the ones from females (Allen, 1880). This results a larger width of the snout and makes it convex on the sides, while in female skulls it is rather straight. The distance between the tusks is smaller by females, resulting in a more slender anterior part of the mandible (Mohr, 1942).

***Figure 4**: Illustration of the size difference between a male (background) and female (foreground) walrus (Lydersen, 2018).*

2.6 Behaviour and reproduction

Walruses are highly gregarious animals. When they are hauled-out, they spend their time resting, huddled together in dense groups to conserve heat (Born et al., 1995; Fay, 1982; Lydersen, 2018). In the summer and fall outside of the breeding season, there is usually no contact between male and female walruses, but the animals live together in large, separated groups of either males or females with

young immature animals (Born et al., 1995; Fay, 1982; Kastelein, 2002; Lydersen, 2018). Females generally start ovulating around the age of seven and usually give birth for the first time when they are about ten years old. Male individuals also become sexually mature around the age of ten, but usually do not get the chance to mate until they are about 15 years old. (Fay, 1982; Kastelein, 2002; Lydersen, 2018).

During the mating season that lasts from January to April, adult males and females gather together. The fertility peak for the older mature bulls lies in December and January, for younger subadult animals about two months later in February and March to reduce competition. Walruses are polygynous animals and the sex ratio in breeding areas during the mating season is about one male per ten females (Born et al., 1995; Fay et al., 1984; Kovacs and Lavigne, 1992; Lindenfors et al., 2002). Intensive fighting between adult males happens in the water in competition for display sites near females. Copulation happens in the water after females have chosen a mate among the displaying males (Born et al., 1995; Fay et al., 1984).

Gestation takes about 15 months, which includes a 4-5 month period of delayed implantation, after which a single calf is born. Females give birth in April and early May on small ice floes apart from the herd. The calves are able to swim immediately after birth and may be carried on their mothers back for a while (Kastelein, 2002; King, 1964; Kovacs and Lavigne, 1992; Lydersen, 2018). They also accompany their mother during feeding excursions. Walrus mothers suckle their calves with relatively low-fat milk for a period of about 2 years, both while onshore and in the water. When the calves reach the age of 5 months, they are strong enough to dive and begin feeding also of benthic organisms. Most calves are weaned by the age of 3, after which the young males join all-male herds and the females assimilate into the mother’s herd. Because of the gestation and long period of maternal care, reproductive females can raise one calf every 3 years (Kastelein, 2002; King, 1964; Kovacs and Lavigne, 1992; Lydersen, 2018).

3 PALEOGEOLOGY AND -GEOGRAPHY OF *HET SCHEUR*

3.1 *Het Scheur* navigation channel

Located in the Southern North Sea Basin on the Belgian Continental Shelf (BCS), *Het Scheur* is a navigation channel directed to the Westerscheldt in the East, where it turns into the Wielingen channel (around the Belgian-Dutch border). It was formed by the incision of river systems during the Pleistocene (De Clercq, 2018). The channel has a depth of 10-12 m, which is maintained by dredging. This dredging activity has caused exposure of older Paleogene and Late Pleistocene sediments. Most of the walrus fossils were collected near the location of the bouy *Scheur 10* (fig. 5).

***Figure 5**: Bathymetric map of the northeast part of the Belgian coast with indication of the location of buoy Scheur 10, where most of the fossils were found. Modified after Post et al. (2017).*

Over the past decades, Dutch fishing activities and targeted surveys have discovered large amounts of mammalian and fish fossil bone material (Post et al., 2017), belonging to different distinct faunas: 1) Middle Eocene (43 Ma) marine fauna (primitive whales and sharks), 2) Late Pleistocene interglacial fauna (aurochs, wild boars, wild horses, red deer, roe deer, rhinoceroses and hippopotamuses), 3) a Late Pleistocene marine/estuarine fauna consisting only of walruses and 4) a glacial Late Pleistocene

fauna (wild horses, bears, red deer) (De Clercq, 2018). A walrus tusk (with an estimated Weichselian age 110-10.5 ka) that was washed up on the beach in 2014 near the city of Ostend (Vermeersch et al., 2015) can probably be related to the walrus fossils from *Het Scheur*, as paleogeographic reconstructions of the Eemian transgression suggest the presence of islands with intertidal flats during the Middle-Late Eemian and Late Eemian at both sides of the Zeebrugge Valley estuary (cfr. 3.3) (De Clercq, 2018).

3.2 Geology of *Het Scheur*

The stratigraphic framework at the location of *Scheur 10* is poor due to the presence of shallow methane gas in the area around Zeebrugge, which prevents seismic penetration into the subsurface. The Paleozoic basement in the area consists of the London-Brabant massive, which is found at about 450 m depth near the Dutch border (Bot et al., 2003). It was not until the Late Cretaceous before the basement got overflown by the sea depositing a chalk layer with the top laying at a depth of about 350 m in the northeast, after which a series of Paleogene, Pleistocene and Holocene sediments were deposited (Bot et al., 2003; Du Four et al., 2006).

3.2.1 Paleogene deposits

Stratigraphic information of the Paleogene strata at the site is correlated with Eocene Maldegem and Zelzate Formations which have generally a constant thickness between the same unit (Bot et al., 2003; De Clercq, 2018; Du Four et al., 2006). These deposits consist of alternations between clay and sand layers. At the location of buoy *Scheur 10*, where most of the fossils were found, there are two Paleogene formations that outcrop on the seafloor (fig 6). West of the Zand Passage, there are two members of the Maldegem Formation (B1b/B1c & B1d) from the middle Eocene. They consist of clay, sandy clay to clayey sand with bioturbations and have a thickness of 45-60 m. In the east lies the Zelzate Formation (P1) from the Upper Eocene, which consists of stiff, slightly sandy clay with a thickness between 40-90 m (Bot et al., 2003; Du Four et al., 2006).

3.2.2 Pleistocene deposits

The Pleistocene deposits consist mainly of infilling of scour holes and paleovalleys. At the southeast side of the channel there's also a quaternary deposit of less than 2.5 m thick, which probably contained the walrus fossils (fig 7 A-B). This deposit may belong to the Eem Formation which consists mainly of fine to very coarse shelly sand with local clay laminae and some gravel (Bot et al., 2003; Du Four et al., 2006).

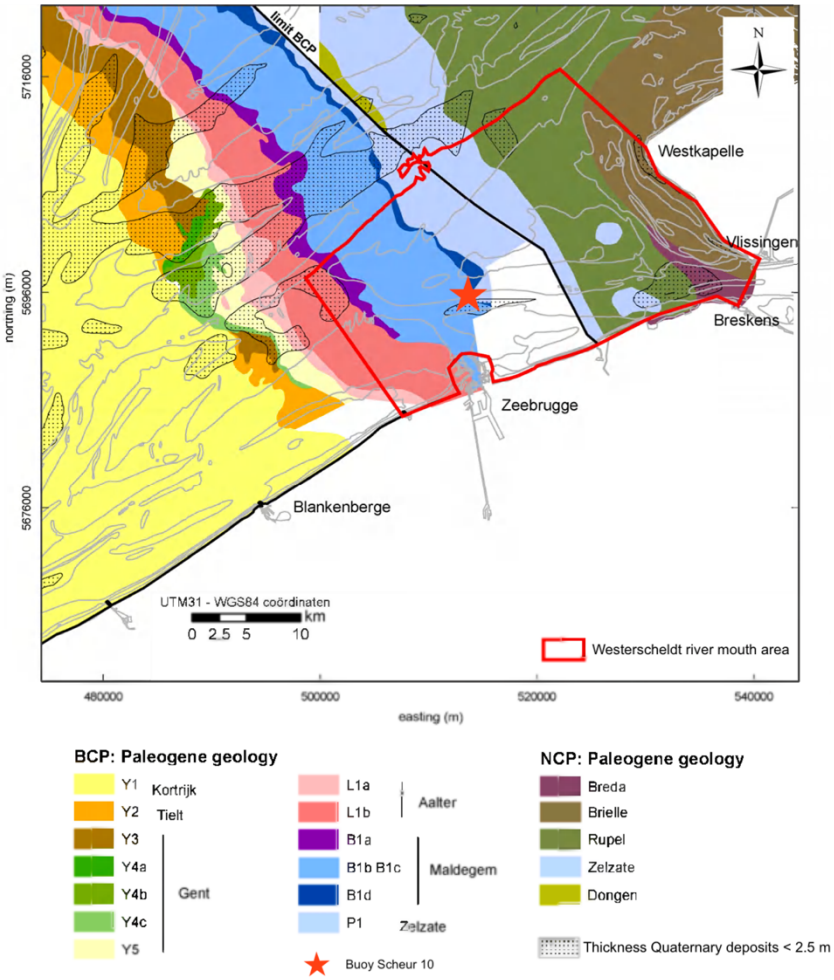

***Figure 6**: Overview of the Paleogene deposits on the northeast Belgian continetal shelf. Data East Modified after Du Four et al. (2006).*

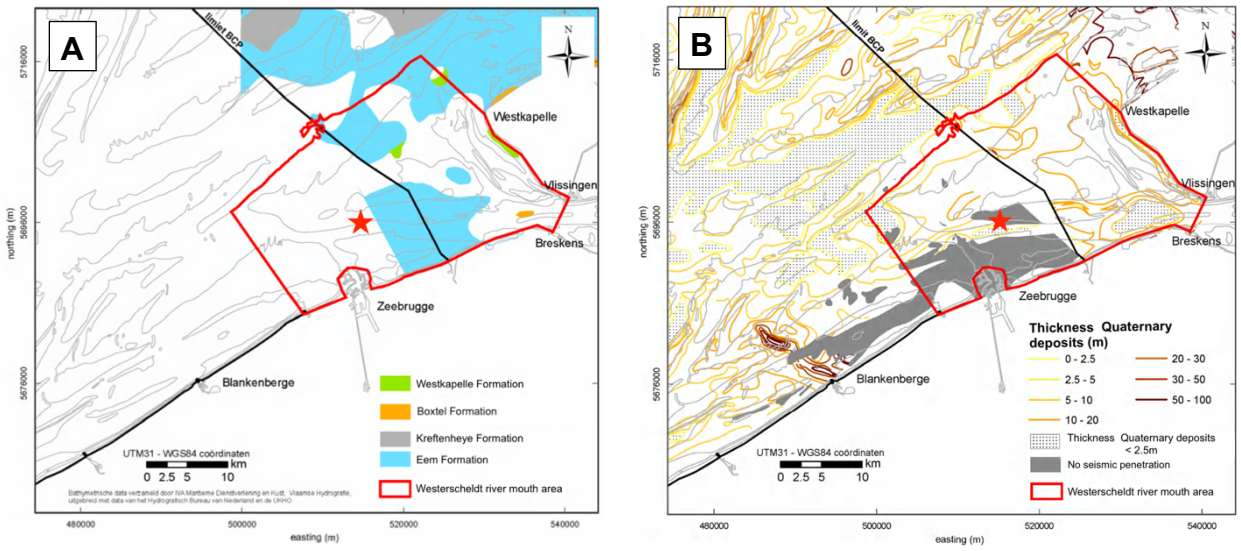

***Figure 5**: A map of the Pleistocene deposits and B map showing the thickness of the Pleistocene deposits and the areas with no seismic penetration. The red star indicates the location of buoy Scheur 10. Modified after Du Four et al. (2006).*

3.2.3 Holocene deposits

The groundwater level rise associated with the sea level rise during the Holocene, caused the formation of a basal peat layer in the coastal areas. In the seaward part of the coastal plain, only brackish and marine sediments were deposited and most of the Pleistocene deposits are eroded and/or reworked into tidal flat sands, estuarine sandbanks and beach deposits. Repeated removing and reworking of fine-grained material during the last part of the Holocene led to the deposition of sand on top of the tidal flat deposits. Holocene sediments mainly consist of medium coarse sands and gravels (Bot et al., 2003; Du Four et al., 2006).

3.3 Paleogeographic reconstruction

3.3.1 Eemian interglacial

After the end of the Saalian glaciation (ca. 126 ka), the climate in western Europe ameliorated, indicating the onset of the Eemian interglacial. The sea level started to rise again from ca. 120 m lower than the present sea level until it reached an eustatic sea-level that exceeded modern levels by at least 5.5 m during high-stand in the Late Eemian (Dutton and Lambeck, 2012; Kopp et al., 2009; Medina-Elizalde, 2013). The Eemian transgression entered the BCS through the Dover strait and extended northward into the southern North Sea between England and Belgium (De Clercq et al., 2018). Recent studies have shown that the Eemian transgression of the BCS took place when the global eustatic sea levels were already dropping and reached high-stand conditions between 115-110 ka. This can be attributed to the glacio-isostatic subsidence of the forebulge between East-Anglia and Belgium after melting of the Fennoscandian and British-Irish Ice Sheets in the North (Cohen et al., 2017, 2012; Lambeck et al., 2012; Long et al., 2015). The high-stand took place at the transition of Marine Isotope Stage (MIS) 5e-d, when the climate was already deteriorating (Vansteenberge et al., 2016; De Clercq, 2018). The rising sea of the Early Eemian transformed the outer BCS to a shallow marine sea and the Offshore Scarp was the paleoshoreline up to the Middle Eemian (fig. 8 A & B). The marine transgression during the Middle Eemian, when the climate gradually started to cool down, resulted in the creation

***Figure 6**: A-H paleoenvironmental reconstructions of the BCS from the beginning of the Eemian (ca. 126 ka) until the Early Holocene (ca. 9.5 ka) with indications of locations of fossils finds. Modified after De Clercq (2018). WMP: western marginal platform, CMP: central marginal platform, EMP: eastern marginal platform, LAT: lowest astronomical tide.*

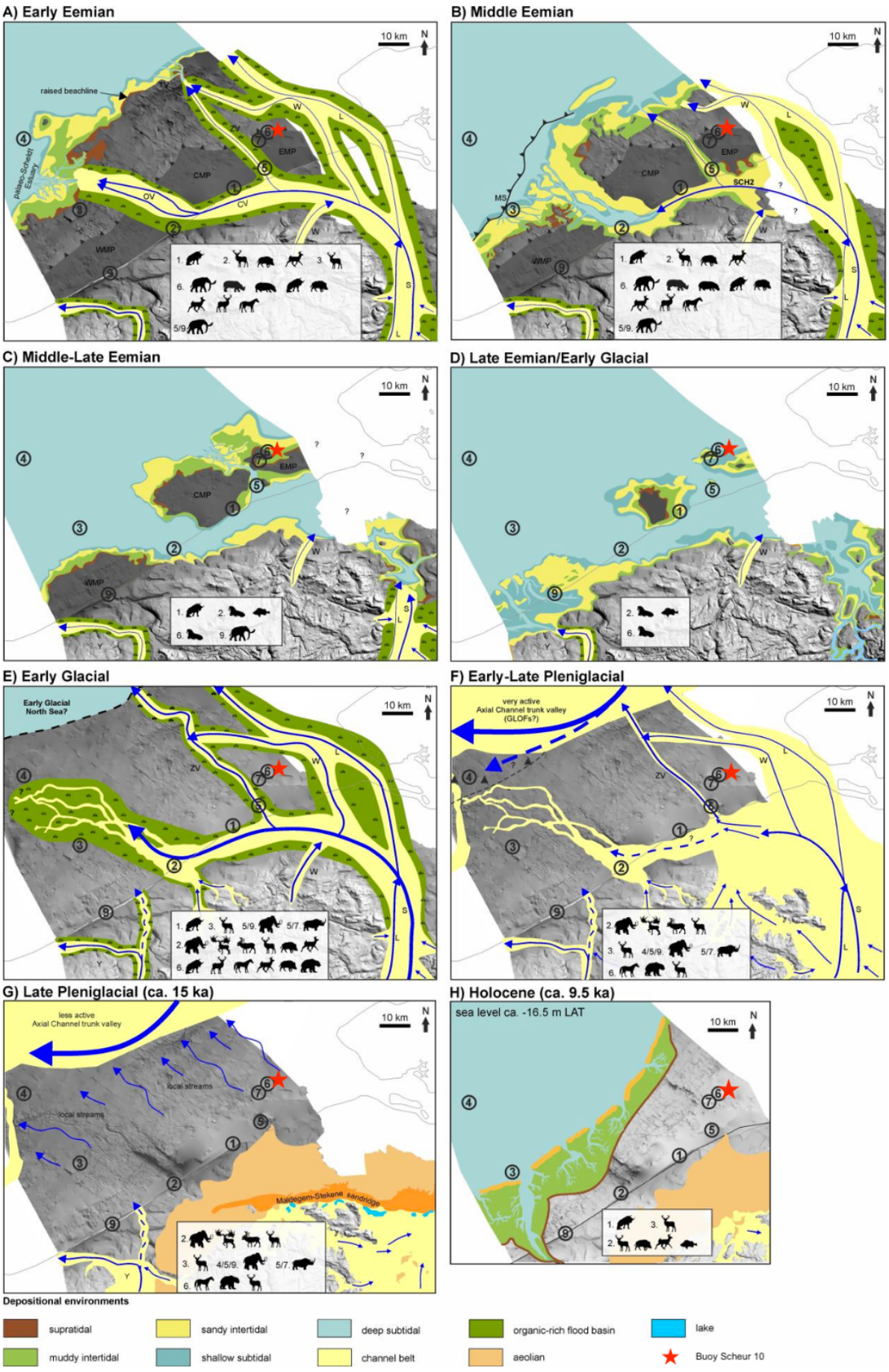
A) Early Eemian
B) Middle Eemian
C) Middle-Late Eemian
D) Late Eemian/Early Glacial
E) Early Glacial
F) Early-Late Pleniglacial
G) Late Pleniglacial (ca. 15 ka)
H) Holocene (ca. 9.5 ka)
10 km
N
raised beachline
Palaeo-Schelde Estuary
CMP
EMP
WMP
OV
CV
ZV
W
L
S
MS
SCH2
Early Glacial North Sea?
very active Axial Channel trunk valley (GLOFs?)
less active Axial Channel trunk valley
local streams
Maldegem-Stekene sandridge
sea level ca. -16.5 m LAT
Depositional environments
supratidal
sandy intertidal
deep subtidal
organic-rich flood basin
lake
muddy intertidal
shallow subtidal
channel belt
aeolian
Buoy Scheur 10

of the intertidal islands on the central and eastern marginal platforms (CMP and EMP) (fig. 8 B). If the climate was already cold enough, it is possible that the walrus occupation in *Het Scheur* could already have been established in the second part of the Middle Eemian.

During the Middle-Late and Late Eemian, islands with intertidal flats were present at both sides of the Zeebrugge valley, which could be a favourable environment for the occupation of a walrus colony (fig. 8 C & D) (De Clercq, 2018).

3.3.2 Weichselian Early Glacial

The climate deteriorated further during the Weichselian and it was characterised by an alternation of colder stadial and warmer interstadial periods (Caspers and Freund, 2001; Helmens, 2014) resulting in a gradual sea level lowering fluctuates between 0 and -60 m relative to present. (Medina-Elizalde, 2013). Sea level information from a global compilation of corals indicates a sea level drop of less than -25 m for the Early Glacial period (116-73 ka), except during the Rederstall stadial when it dropped to -60 m. The paleogeographic reconstruction in figure 8 E-G shows that during this time, as well as during the Pleniglacial, the area of *Het Scheur* was located too far landward from the retreated paleoshoreline to be occupied by a walrus colony.

3.4 Taphonomy and dating of the fossils

The exceptional preservation of most of the fossils as well as fragile material such as the preservation of teeth within the jawbone, may suggest *in situ* preservation. This is also indicated by the presence of a clean side and a side which was covered with living barnacles and bryozoans due to exposure to the seawater for a certain time.

Since the fossils were collected by beam trawling, no accurate stratigraphic context is available. Radiocarbon dating that was performed on some bone fragments, yielding an ambiguous age of at least 45 to 50 ka, close to the limit of this dating technique (Missiaen et al., 2019; Seys, 2017), which is similar to other *Odobenus* fossils from the Netherlands (Post, 1999). This age seems implausible as the site where the fossils were found is thought to be distant to the shore at that time. Recent paleogeographic reconstructions by De Clercq (2018) rather suggest a late Eemian-Early Glacial origin. To solve this question, a number a sediment cores were taken along the coastline in the summer of 2018 (Missiaen et al., 2019; Seys, 2017) There has also been planned to take shallow sediment cores at the site and to

perform additional dating based on shell residue and climate proxies (diatoms, dinoflagellates and pollen). This research is still on-going and results were not yet available.

4 MATERIALS AND METHODS

4.1 Biological and paleontological samples

A total of 43 specimens were available for measurement, representing different parts of the walrus skeleton. All the specimens, except for the almost complete skull (IRSNB-06498-3228), were recently collected at *Het Scheur* navigation channel off the Belgian coast by bottom trawling during several campaigns by the NMR in 2015-2016 and together with the VLIZ in 2017 and 2018, together with material of other Pleistocene megafauna such as whales, aurochs and giant deer (Hablützel et al., 2018; Langeveld, 2018; Post et al., 2017). The specimens collected by the VLIZ are now curated at the Royal Belgian Institute of Natural Sciences (IRSNB). A preliminary identification of the fossils as *Odobenus rosmarus* bones was made by Bram Langeveld (NMR), based on their characteristic morphologies and large sizes. The skull IRSNB-06498-3228 from the IRSNB collection was washed up on the coast and found on the beach of Heist in 1897, as is written on the label of the specimen. An overview of all the specimens is given in table 1.

A complete skeleton (without tusks) of an adult female (IRSNB 1150B) and a skull of an adult male (IRSNB 1150D) of recent Atlantic walruses from the collection of the IRSNB were at our disposal for comparison of the different bones.

***Table 1**: List of all the studied specimens.*

Collection number	***Type***	***Date of collection***
IRSNB-06498-3228	skull	27/10/1897
IRSNB-34228-032	skull	11/01/2018
IRSNB-34228-033	pelvis	July 2017
IRSNB-34228-034	mandible	July 2017
IRSNB-34228-035	mandible	11/01/2018
IRSNB-34228-036	mandible	11/01/2018
IRSNB-34228-037	lumbar vertebra fragment	31/07/2017
IRSNB-34228-038	cuboid bone	10/01/2018
IRSNB-34228-039	cervical vertebra fragment	July 2017
IRSNB-34228-040	femur	11/01/2018
IRSNB-34228-041	skull fragment	09/01/2018
IRSNB-34228-042	skull fragment	09/01/2018
IRSNB-34228-043	skull fragment	11/01/2018
IRSNB-34228-044	humerus	July 2017
IRSNB-34228-045	radius	10/01/2018
IRSNB-34228-046	humerus	10/01/2018
IRSNB-34228-047	rib	09/01/2018
IRSNB-34228-048	rib	July 2017
IRSNB-34228-049	tusk	10/01/2018
IRSNB-34228-050	rib	11/01/2018
IRSNB-34228-051	ulna	11/01/2018
IRSNB-34228-052	rib	July 2017
IRSNB-34228-053	rib	July 2017
IRSNB-34228-054	rib	09/01/2018

IRSNB-34228-055	rib	11/01/2018
IRSNB-34228-056	indeterminate fragment	July 2017
IRSNB-34228-057	lumbar vertebra	11/01/2018
IRSNB-34228-058	costa	09/01/2018
IRSNB-34228-059	pelvis fragment	09/01/2018
NMR999100012536	pelvis	January 2015
NMR999100012537	radius	January 2015
NMR999100013792	ulna	09/09/2016
NMR999100014070	femur	09/09/2016
NMR999100014071	humerus	09/09/2016
NMR999100014072	thoracic vertebra	09/09/2016
NMR999100014073	rib	09/09/2016
NMR999100014074	rib	09/09/2016
NMR999100014075	rib	09/09/2016
NMR999100016478	rib	June 2017
NMR999100016479	thoracic vertebra	June 2017
NMR999100016480	thoracic vertebra	June 2017
NMR999100016764	radius	April 2018
NMR999100016797	skull	January 2016

Recent and fossil *Odobenus* specimens from the literature that are used for comparison of the fossils are described by Mohr (1942), Harington (1975), Bisaillon and Piérard, (1981), Erdbrink and van Bree, (1986, 1999a, 1999b), Harington and Beard (1992) and Wiig et al. (2007). Table 2 displays an overview of the institutional abbreviations of all the specimens from the literature that are used.

Table 2: *Explanation of all the institutional abbreviations of samples from the literature that are used.*

Abbreviation	***Institution***
IRSNB	Royal Belgian Institute of Natural Sciences, Brussels, Belgium
NMR	Museum of Natural History Rotterdam, Rotterdam, the Netherlands
ZMA	Zoological Museum of the University of Amsterdam, Amsterdam, the Netherlands
St.	Naturalis, Leiden, the Netherlands
NFM	Newfoundland Museum, St. John's, Canada
NMC	Canadian Museum of Nature, Ottawa, Canada
KP	Collection Klaas Post (private collection), Klifweg 6, 8321 EJ Urk, The Netherlands
N.Z.	Collection Stolzenbach (private collection), Regent Smisstraat 24, Sint-Michielsgestel, The Netherlands
VMUM	Museum of the Anatomy Laboratory of the faculty of Veterinary Medicine of the University of Montreal, Montreal, Canada
ZMH	Zoologisches Museum für Hamburg, Hamburg, Germany

4.2 Measurements

The sizes of the characteristic features on each bone are measured with a mechanical caliper with a 0.1 mm accuracy and they are compared with known specimens from the literature. Because not every researcher used the same terminology for each measurement or the direction of measuring, comparing measurements from different researchers, especially from older literature, could be somewhat confusing. Therefore, I tried to use the most standard terminology and measurements of the different

researchers are converted to be able to compare the investigated fossils with the different specimens known form the literature. The terminology used in the present study is adopted from the terminology employed by Bisaillon and Piérard (1981, 1983) and Committee on Marine Mammals (1967). To avoid any disambiguation about the exact measurements, the most important measurements that are conducted are indicated on the following figures and listed in consecutive tables, each with an own code that starts with the first letter of the bone: the skull (fig. 9, table 3), the mandible (fig. 10, table 4), the vertebra (fig. 11, table 5), the humerus (fig. 12, table 6), the radius and ulna (fig. 13, table 7), innominate (fig. 14, table 8), and femur (fig.15, table 9).

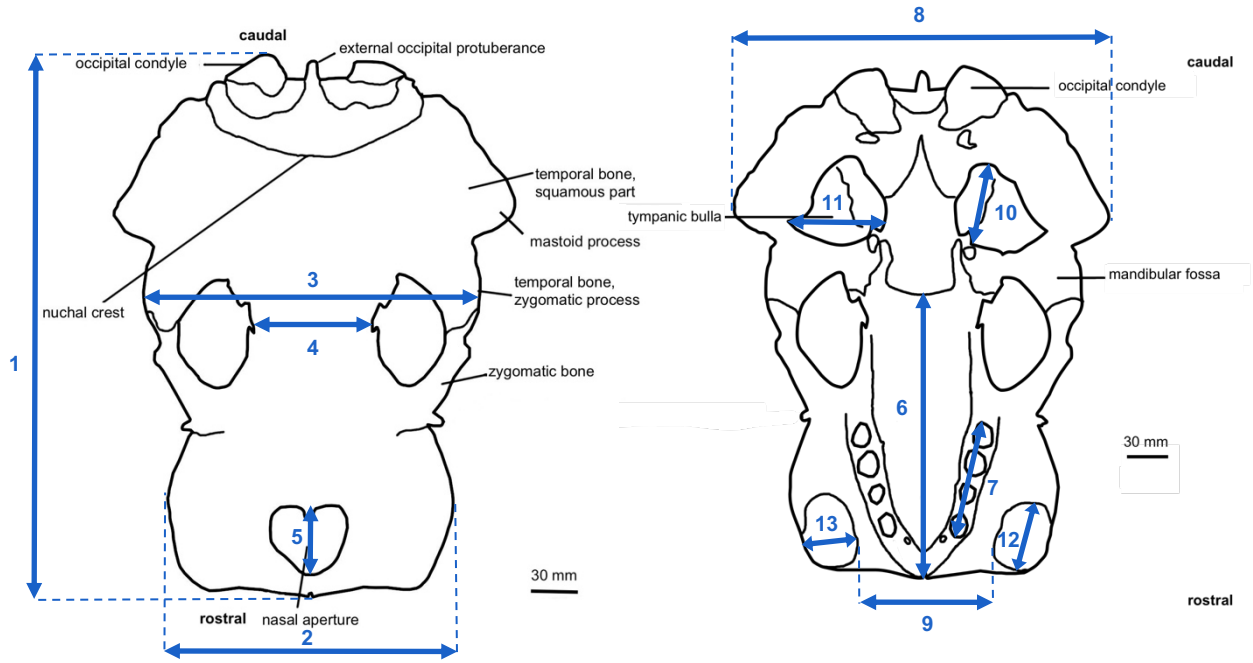

***Figure 7**: Dorsal (upper) and ventral (lower) view of a walrus skull.*

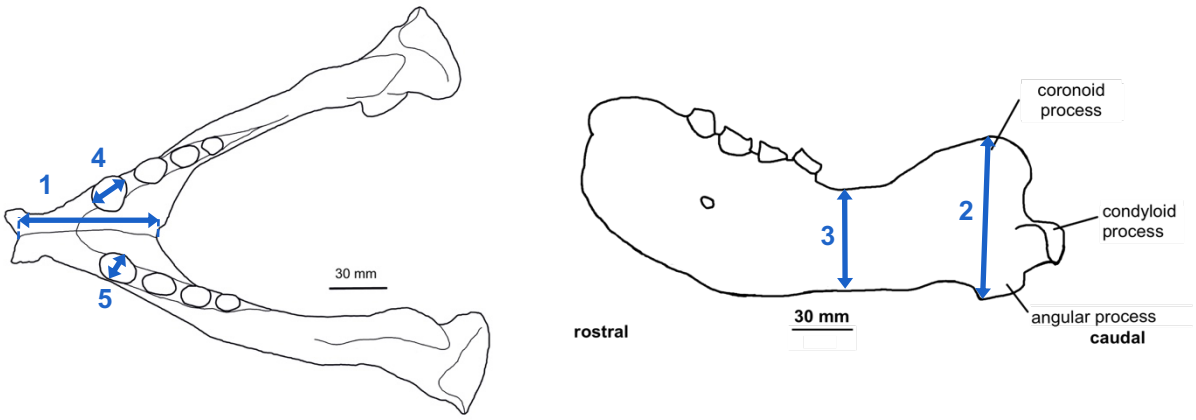

***Figure 8**: Occlusal (left) and lateral (right) view of a mandible.*

Table 4: Measurements of the skull.

S1	condylobasal length	**S8**	cranial width posterior to the zygomatic arches
S2	max. rostral width	**S9**	inner distance between tusk alveoli
S3	max. zygomatic width	**S10**	max. rostro-caudal width of the tympanic bulla
S4	min. interorbital width	**S11**	max. transversal width of the tympanic bulla
S5	dorsoventral diameter of the nasal aperture	**S12**	max. rostro-caudal diameter of the canine alveolus
S6	palatal length	**S13**	min. transversal diameter of the canine alveolus
S7	alveolar length I^3-P^3		

Table 3: Measurements of the mandible.

M1	symphysis length
M2	mandible height
M3	least mandible depth
M4	rostro-caudal diameter of the C_1 alveolus
M5	transversal diameter of the C_1 alveolus

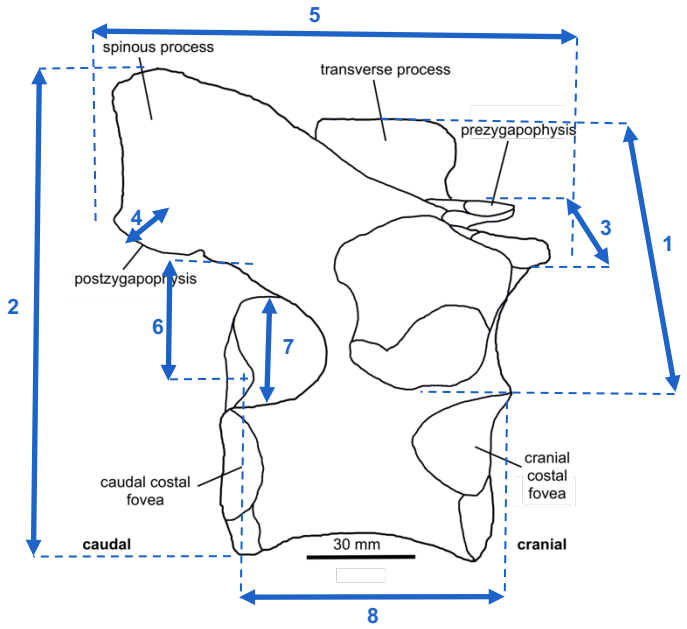

Figure 9: Right side view of the 7th thoracic vertebra.

Table 5: Measurements of the vertebra.

V1	width over the transversal processes
V2	max. total height
V3	transversal length over the prezygapophyses
V4	transversal length over the postzygapophyses
V5	antero-posterior length over the zygapophyses
V6	height of the neural canal
V7	max. width of the neural canal
V8	basal length of the neural canal

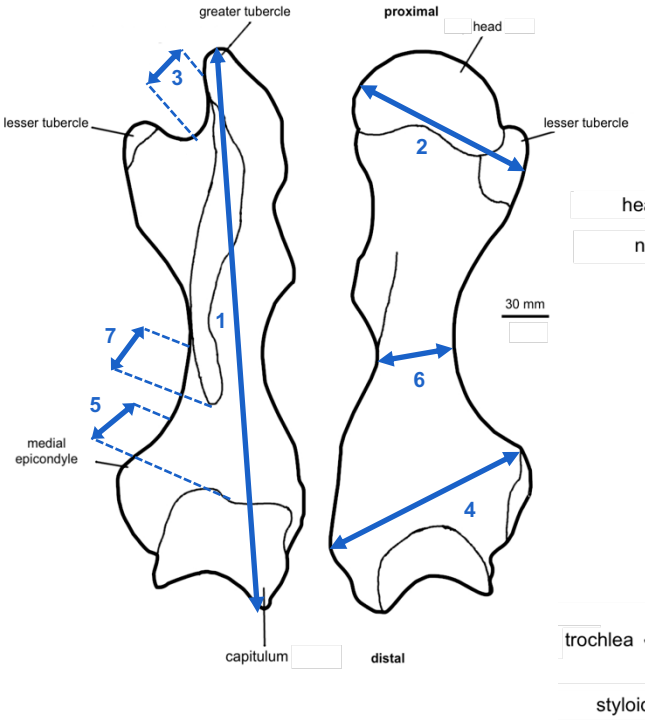

Figure 12: Cranial (left) and caudal (right) view of a left humerus.

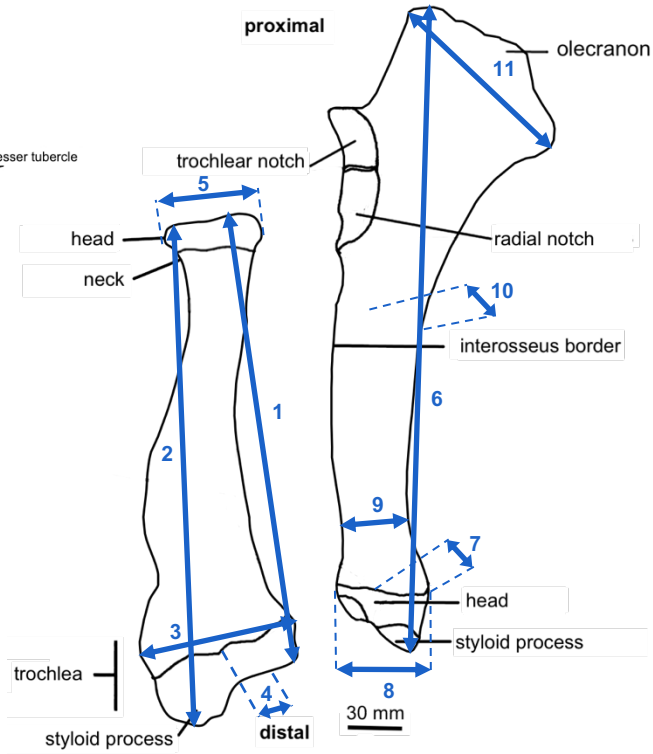

Figure 10: Lateral view of a left radius (left) and ulna (right).

Table 6: Measurements of the humerus.

H1	max. length
H2	transversal proximal width
H3	sagittal proximal width
H4	transversal distal width
H5	sagittal distal width
H6	min. transversal width at the centre of the diaphysis
H7	sagittal width at the centre of the diaphysis
H8	min. circumference of the diaphysis*

Table 5: Measurements of the radius (R1-5) and ulna (R6-11).

R1	length along ulnar side	**R6**	max. length of the ulna
R2	length along posterior side over the crest	**R7**	max. transversal distal width
R3	max. transversal distal width	**R8**	max. sagittal distal width
R4	max. sagittal distal width	**R9**	min. transversal width of the diaphysis
R5	max. proximal width	**R10**	min. sagittal width of the diaphysis
		R11	length over the olecranon

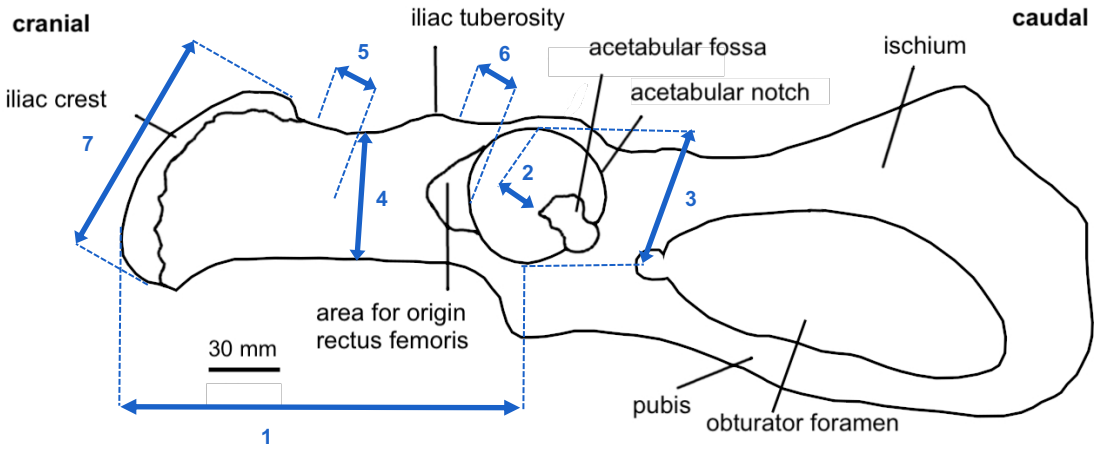

Figure 12: Lateral view of a left innominate.

*Table 7: Measurements of the pelvis. *not indicated.*

P1	max. length of the ilium
P2	max. depth of the acetabulum
P3	diameter of the acetabulum at right angles of the direction of the obturator foramen
P4	min. width of the iliac column
P5	min. height of the iliac column
P6	thickness of the bone at the edge of the acetabulum
P7	width over the iliac crest
P8	min. circumference of the iliac column*

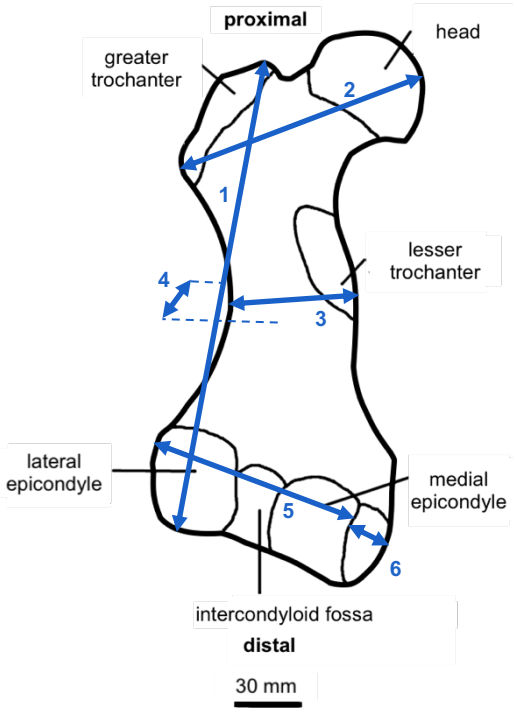

Figure 11: Caudal view of a left femur.

*Table 6: Measurements of the femur. *not indicated.*

F1	max. length over the greater trochanter
F2	max. proximal width (head-greater troch.)
F3	transversal min. width over the centre of the diaphysis
F4	sagittal min. width over the centre of the diaphysis
F5	transversal width over the condyles
F6	sagittal width over the condyles
F7	circumference at the centre of the diaphysis*

5 RESULTS

5.1 Skull

Six skull fragments are available for this study. The measurements that were taken are presented in table 10. Specimen NMR 999100016797 (fig. 16) comprises a large part of the rostrum with the nasal aperture, half of the canine alveoli and part of the palate with all the teeth. The fissure between the premaxilla is wide and the nasal spine is well-pronounced. Most of the sutures such as the sagittal and the nasomaxillary suture are fused and not visible anymore. The majority of the teeth of the specimen are still present. The tooth formula for the upper jaw is here I^{2-3} C^{1} Pm^{1-3}. Neither left nor right Pm^{3} are preserved; only the alveoli are present. On the left side, there is also the occurrence of a vestigial alveolus of Pm^{4}. I^{2} are generally considered rudimentary teeth and disappear in most of the old adult animals (Kryukova, 2012). The fact that they are still present in this specimen, together with the large fissure between the premaxilla, might indicate that the animal was still not yet fully grown. The inner distance between the tusk alveoli has been shown by Mohr (1942) (table in appendix) to be a robust indicator for sexual dimorphism by adult animals. Based on this characteristic, specimen NMR 999100016797 was probably a subadult female.

Specimen IRSNB-06498-3228 (fig. 17) is an almost complete skull with both tusks that washed up on the beach. The only parts that are missing are the occipital condyles. In contrast to NMR 999100016797, the fissure between the premaxilla is closed and the nasal spine does not contrast much from the surrounding bone. The nuchal crest is well-developed, indicating an older age (adult) (Kastelein and Gerrits., 1990). The preserved teeth in the upper jaw are: I^{3}, C^{1}, Pm^{1}, Pm^{2} and Pm^{3}. The left Pm^{3} is lost and only its alveolus is present. There are also some small alveoli of rudimentary teeth I^{2}, Pm^{4}, and M^{1} present that have been lost while growing up. The tusks are still present and rather small in comparison with the dimension of the skull. Much of the outer bone layer of the tusks has been removed by abrasion. The outer sides of the alveoli of the tusks are convex, causing a larger width of the rostrum, a typical characteristic for male individuals (Mohr, 1942). This is confirmed looking at the condylobasal length and the inner distance between the tusks.

The skull specimen with number IRSNB-34228-032 (fig. 19 H) is a part of the nuchal crest and external occipital protuberance (*protuberantia occipitalis externa)*. The ridges of the parietal bone are also well visible. The large development of the nuchal crest suggests that it was an adult animal. The interparietal

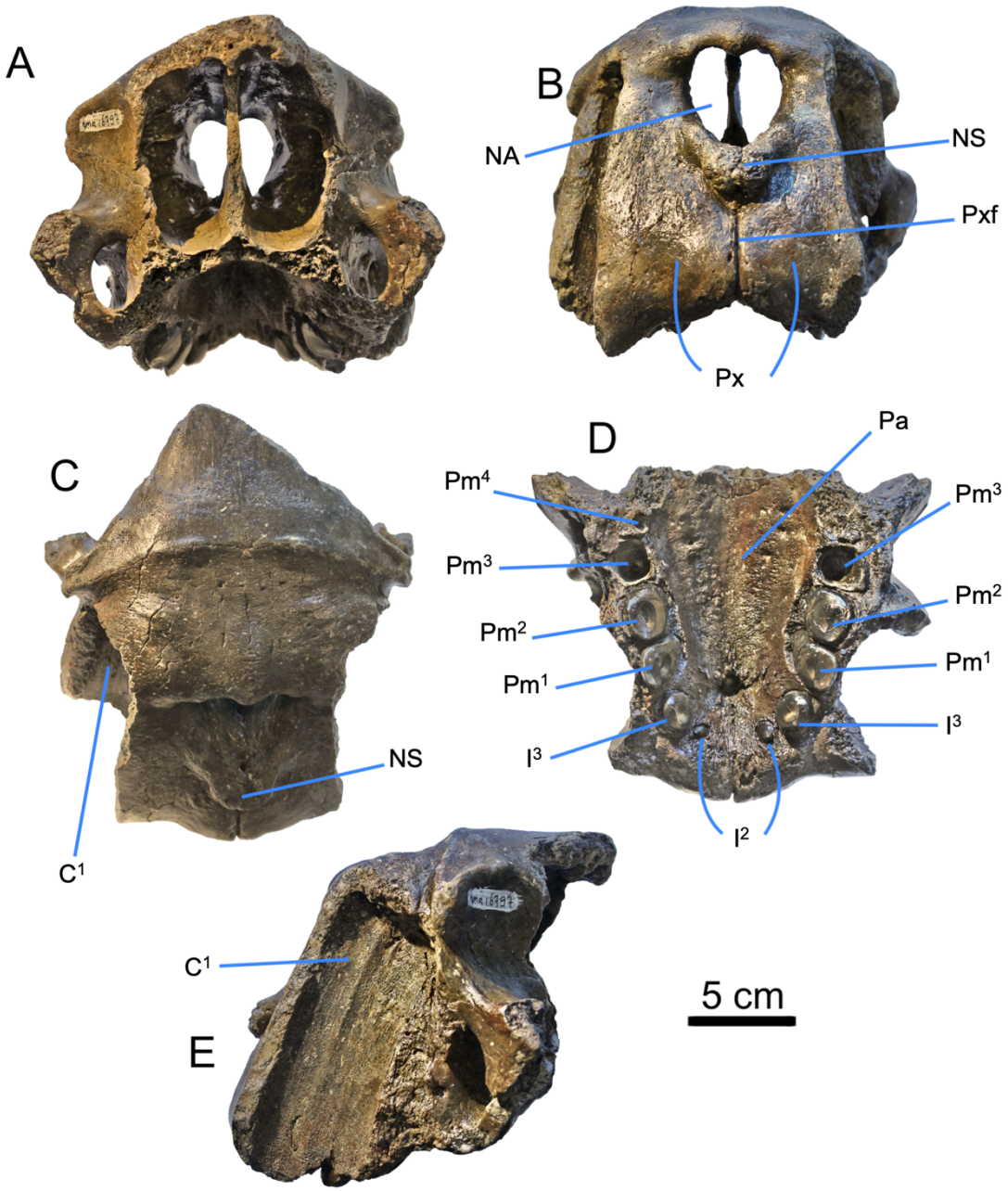

***Figure 13**: A-E respectively caudal, rostral, dorsal, ventral and left side view of the skull with number NMR999100016797. C^1 canine (tusk); I^{2-3} incisor teeth; Pm^{1-3} premolar teeth; NA nasal aperture; NS nasal spine; PX premaxilla bones; Pxf premaxilla fissure.*

region is depressed and the parietointerparietal sutures form distinct ridges. The interparietal bone is significantly smaller than compared to skulls of other adult male walruses described by Kastelein and Gerrits (1990) and IRSNB-1150D from the IRSNB collection. Therefore, it might represent an adult female walrus.

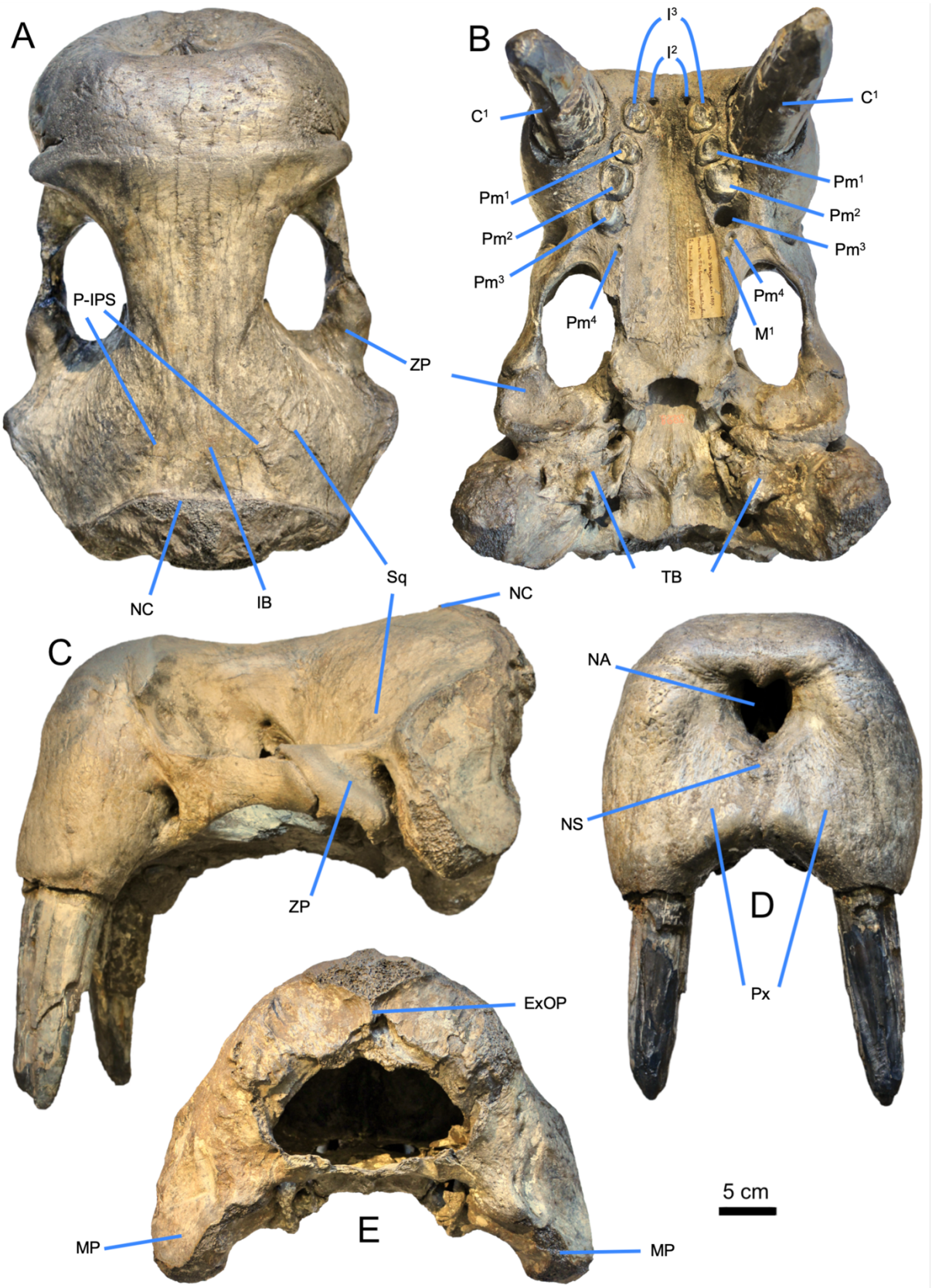

***Figure 14**: A-E respectively caudal, rostral, dorsal, ventral and left side view of the skull with number IRSNB-06498-3228. C^1 canine (tusk); I^{2-3} incisor teeth; Pm^{1-4} premolar teeth; M^1 molar teeth; ExOP external occipital protuberance; IB interparietal bone; P-IPS parietointeparietal suture; MP mastoid process; NC nuchal crest; NA nasal aperture; NS nasal spine; PX premaxilla bones; Pxf premaxilla fissure; Sq squamosum; TB tympanic bulla; ZP zygomatic process.*

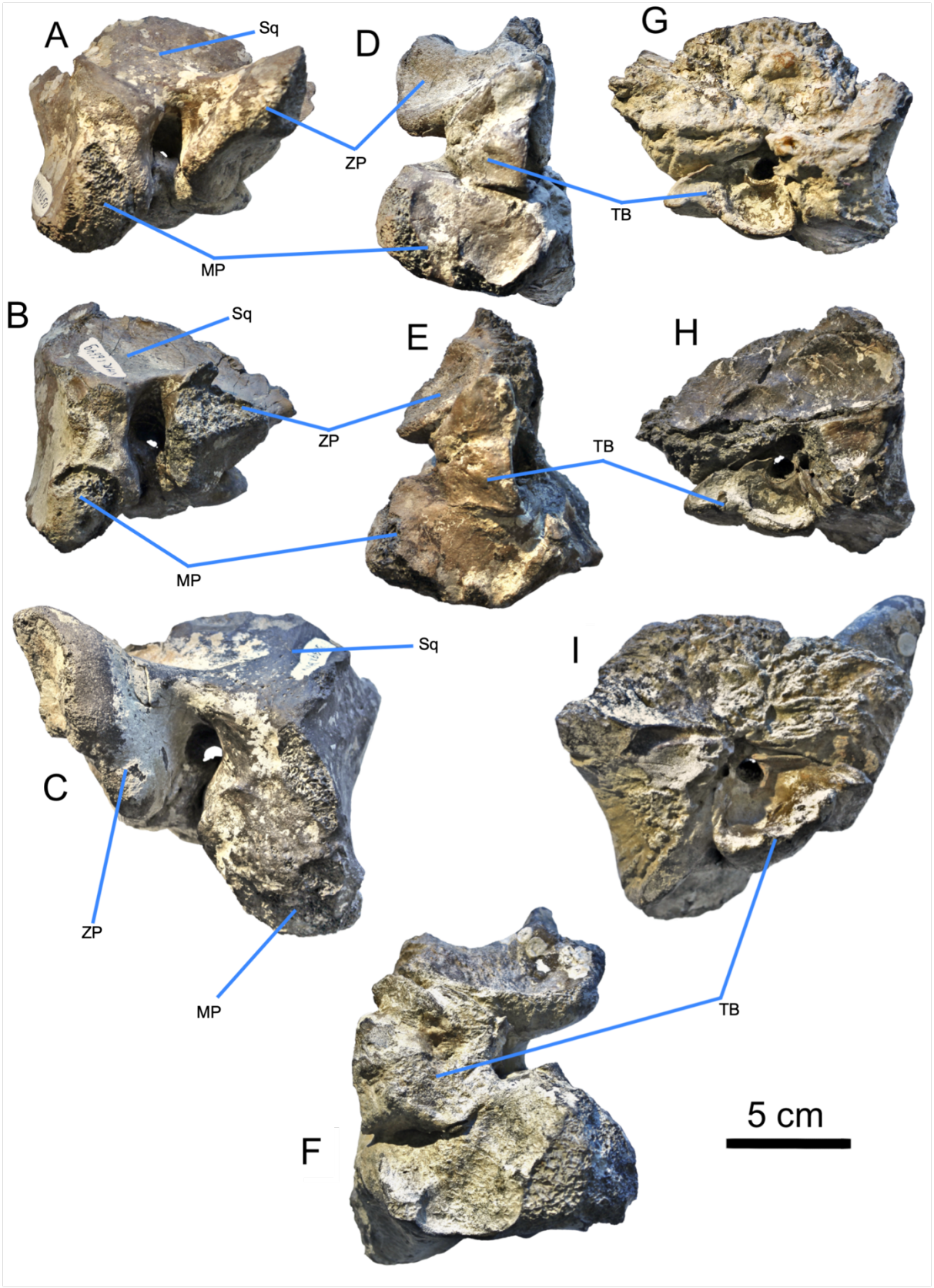

***Figure 15**; A-I respectively lateral, ventral and medial aspect of two right (IRSNB-34228-041 & IRSNB-34228-042) and one left (IRSNB-34228-043) temporal bone. MP mastoid process; TB tympanic bulla; Sq squamosum; ZP zygomatic process.*

Specimens IRSNB-34228-041, IRSNB-34228-042 and IRSNB-34228-043 are respectively two right and one left temporal bone (fig. 18). They all consist of the squamosum, mastoid process and tympanic bulla (*bulla tympanica)*. The zygomatic process is only preserved in IRSNB-34228-041, IRSNB-34228-042. The identification of the remains of the three temporal bones is based on the size of the tympanic bulla. In all three specimens, part of the tympanic bulla is broken off at the medial side, which means that the measurement of the max transversal width will give an underestimation of the size. In the rostro-caudal direction on the other hand is the tympanic bulla more or less complete. The fossils are compared with the skulls of a recent adult male (IRSNB-1150D) and female (IRSNB-1150B) from the IRSNB collection. IRSNB-34228-043 is the largest of the three temporal bones and has a well-developed mastoid process. The length of its tympanic bulla is larger than in the female skull and similar to the male skull, hence it was probably from an adult male. The right temporal bones IRSNB-34228-041 and IRSNB-34228-042 are significantly smaller in size. Their tympanic bulla is slightly smaller than the female skull. In both specimens is the mastoid process small and is almost not ventrally developed, which suggests that they were most likely juvenile animals.

5.2 Mandible

Specimens IRSNB-34228-034, IRSNB-34228-035 and IRSNB-34228-036 (fig. 19 A-G) are mandibular fragments. IRSNB-34228-034 is the posterior part of a left ramus, around the coronoid, extending almost to the lowest part of the mandible. The condyle is broken off and the angular process also shows abrasion damage. The coronoid crest is wide and has a rather gradual incline on the rostral side. Wiig et al. (2007) and Taylor et al. (2020) proved that size measurements of mandibles, such as the least mandible depth and the mandible height of mature individuals can be a reliable method to determine the sex. If we compare those measurements with this specimen, IRSNB-34228-034 represents most likely a subadult male.

The other two specimens are parts of the anterior of the mandible with the left and right alveoli of C_1 present and for specimen IRSNB-34228-036, the right C_1 is also preserved. IRSNB-34228-035 also shows parts of the alveoli of the first premolars on both sides. The symphysis between both rami of IRSNB-34228-035 is not fully fused and the curvature is slightly convex with a broad anterior end of the mandible. On IRSNB-34228-036 is the suture of the symphysis completely fused and not visible anymore. The symphysis line is rather straight and the mandible is narrow at its most anterior point.

***Table 8**: Measurements of the skull(fragments) (names in bold) in mm compared with a recent male and female walrus from the IRSNB collection.*

	NMR 999100016797 (L/R)	***IRSNB 06498-3228 (L/R)***	***IRSNB 34228-041***	***IRSNB 34228-042***	***IRSNB 34228-043***	*IRSNB 1150D (L/R)*	*IRSNB 1150B*
Sex (M/F/J)						M	F
S1 condylobasal length	/	> 390	/	/	/	375	325
S2 max. rostral width	/	221	/	/	/	195	144
S3 max. zygomatic width	/	251	/	/	/	238	209
S4 min. interorbital width	/	87	/	/	/	85	54
S5 dorsoventral diameter of the nasal aperture	38	35	/	/	/	35	33
S6 palatal length	> 130	225	/	/	/	196	188
S7 alveolar length I^3-P^3	73.6/73.5	96/95	/	/	/	92/94	70
S8 cranial width posterior to the zygomatic arches	/	± 299	/	/	/	290	253
S9 inner distance between tusk alveoli	74	86	/	/	/	91	75
S10 max transversal width bulla tympanica	/	82/83	> 43	> 42	> 52	71	58
S11 max rostro-caudal length bulla tympanica	/	63/65	± 48	± 50	± 58	59	53
S12 rostro-caudal diameter canine alveolus	43	64	/	/	/	64	59

***Table 9:** Measurements in mm of the tusk (name in bold) compared with specimens described by Harington (1975).*

	IRSNB 34228-049	*NMC 32384*	*NMC 32376*	*NMC 32377*	*NMC 32352*	*NMC 32321*	*NMC 32375*	*NMC 32323*	*NMC 32317*	*NMC 32303*
Sex (M/F/J)		M	F	F	M	M	M	M	M	F
Age (years)		7.2	8.2	8.2	8.3	9.3	10.2	12.2	15.2	22.2
max length (root to tip)	331	273	306	295	330	290	360	385	420	446
max circumference	168	106	107	108	129	118	132	139	164	114
anteroposterior diameter at root	61	23.2	24.5	25.5	27.3	27.3	30.3	31	37.7	26.9
mediolateral diameter at root	36	38.2	36.9	37	47.8	43.5	48.6	49	57.7	41.2

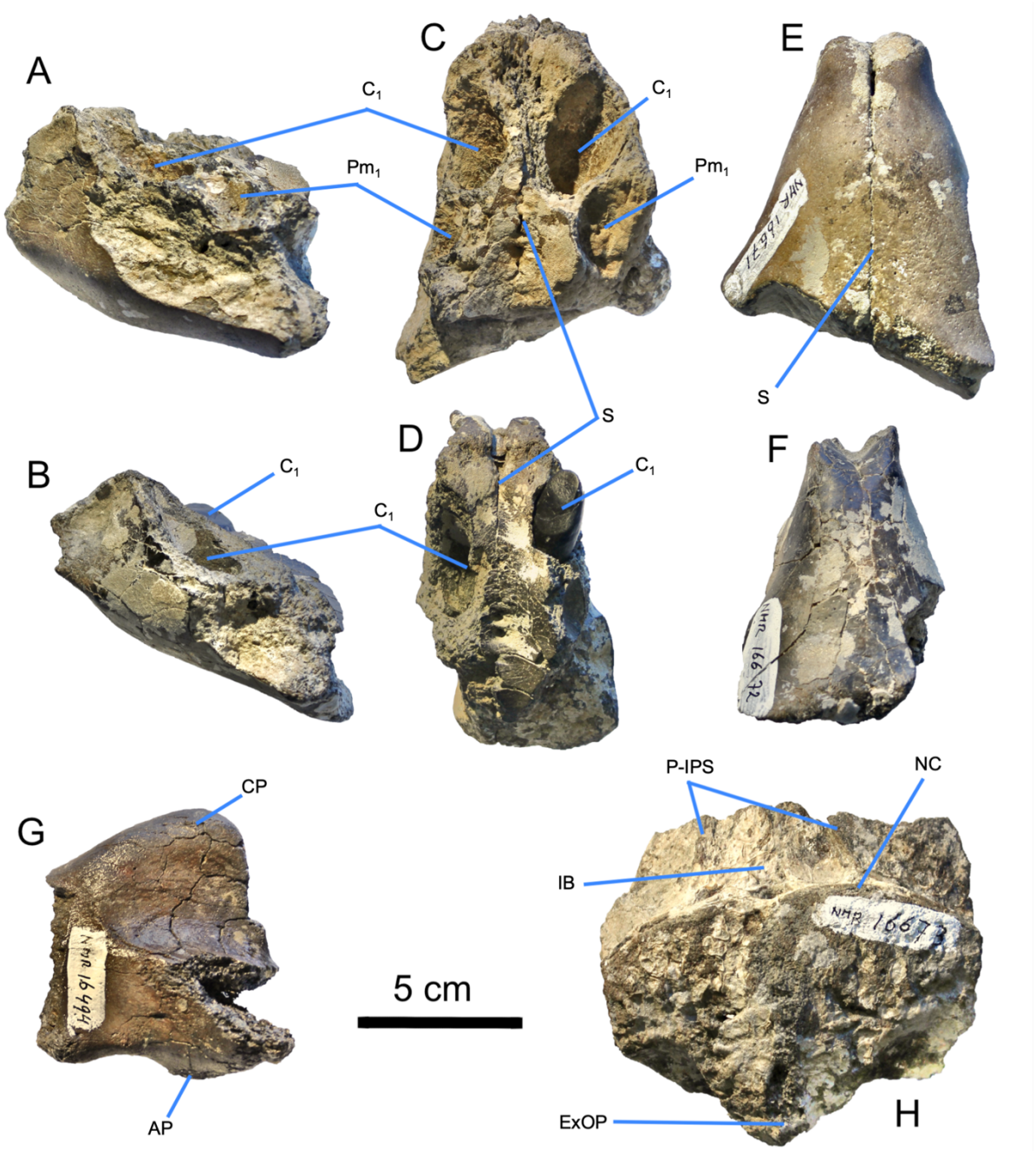

***Figure 16**: A-F respectively lateral, occlusal and ventral aspect of mandibles IRSNB-34228-035 and IRSNB-34228-036. G lateral view of a posterior part of a the left ramus of mandible IRSNB-34228-034. H caudal part of a skull with number IRSNB-34228-032. AP angular process; CP coronoid process; IB interparietal bone; NC nuchal crest; P-IPS parietointerparietal suture; ExOP external occipital protuberance; C_1 lower canine; Pm_1 lower premolar; S symphysis.*

These two specimens have suffered too much from abrasion damage to apply any of the measurements studied by Wiig et al. (2007) and Taylor et al. (2020). The partly fused symphysis of IRSNB-34228-035 indicates that it is still a subadult. Based on the comparison of the alveolar diameters of the specimens with the mandibles IRSNB 1150 B & D, together with descriptions of the symphysis curvature by Mohr

(1942), IRSNB-34228-035 possibly belongs to a subadult male and IRSNB-34228-036 to an adult female. Measurements of these specimens can be found in table 10.

***Table 10**: Measurements in mm of the mandibles (names in bold) compared mean measurements of recent male (n = 32) and female (n = 23) Atlantic walruses made by (Wiig et al., 2007).*

	IRSNB 34228-034	***IRSNB 34228-035***	***IRSNB 34228-036***	*IRSNB 1150D (L/R)*	*IRSNB 1150B (L/R)*	*Mean recent walruses*	
Sex (M/F/J)				M	F	M	F
Age						adult	adult
M1 symphysis length	/	93.4	89.9	98.5	80.4	/	/
M2 coronoid height	> 80.8	/	/	81.0/81.8	76.7/78.7	88.61 ± 5.21	75.27 ± 4.37
M3 least mandible depth	< 56.7	/	/	56.4/56.6	47.6/47.1	59.2 ± 3.52	47.36 ± 3.0
M4 rostro-caudal diameter of the C_1 alveolus							
C_1R	/	± 21.0	19.0	22.5	17.0	/	/
C_1S	/	± 22.0	± 18.8	21.9	16.7	/	/
M5 transversal diameter of the C_1 alveolus							
C_1R	/	± 17.7	13.4	16.5	11.6	/	/
C_1S	/	± 16.4	± 13.1	16.9	11.2	/	/

5.3 Tusk

Specimen IRSNB-34228-049 (fig. 20) is a complete tusk. It had been damaged, which caused it to lose part of the outer bone layer. This specimen is also sampled in for DNA analysis in the study mentioned before. The left side of the tusk is flatter, while the right side is more convex. The tusk is also slightly curved towards the right. The two large longitudinal grooves that are present on the left side possibly suggest that it is the right tusk. This tusk was compared with the ones described by Harington (1975), where he focussed mainly on the measurements of the total length and the mediolateral and anteroposterior diameter of the tusk at the alveolar margin. The exact mark of the alveolar margin is not visible on this tusk. However, the tusk does not show great differences in diameter from the bottom of the root up to the middle. The large diameter of the tusk might indicate that it was an adult male individual. Measurements of the tusk are listed in table 11.

***Figure 17**: A-B left and right side view of a tusk with number IRSNB-34228-049. The arrows indicate two longitudinal grooves which may indicate the medial side.*

5.4 Vertebra

Six vertebrae were also available for this study. All the measurement that are taken are presented in table 13. The specimen IRSNB-34228-039 (fig. 21 G-H) is just a fragment of a vertebra. The surface where the collection number is indicated, is clearly a postzygapophysis plane. Compared to the vertebra of the female skeleton IRSNB-1150B, it shows the greatest resemblance to right postzygapophysis of the 6thor the 7th cervical vertebra. The bone fragment is with a width of 33 mm over the postzygapophysis substantially larger than the width of 26 mm of the female vertebra. This could suggest that it might be from a male individual. But it is not certain as there were no male vertebra available for comparison. Specimens NMR 999100014072, NMR 999100016480 and NMR 999100016479 (fig. 21 A-F) are thoracic vertebrae. Specimen NMR 999100014072 is heavily damaged, all the processes are lost and only the vertebral body is preserved. The convex cranial articular surface is still present, but the concave caudal articular surface is eroded away. Based on its size and the direction of the placement of the cranial costal foveae (*foveae costalis cranialis)*, it might possibly be a 4th or the 5th thoracic vertebra. The fossil is too damaged to be able to identify the sex of the animal. The specimen that bears the name NMR 999100016480 is much better preserved. The prezygapophyses (*zygapophysis cranialis*) are only partly preserved and the postzygapophyses (*zygapophysis caudalis*), together with the spinous process

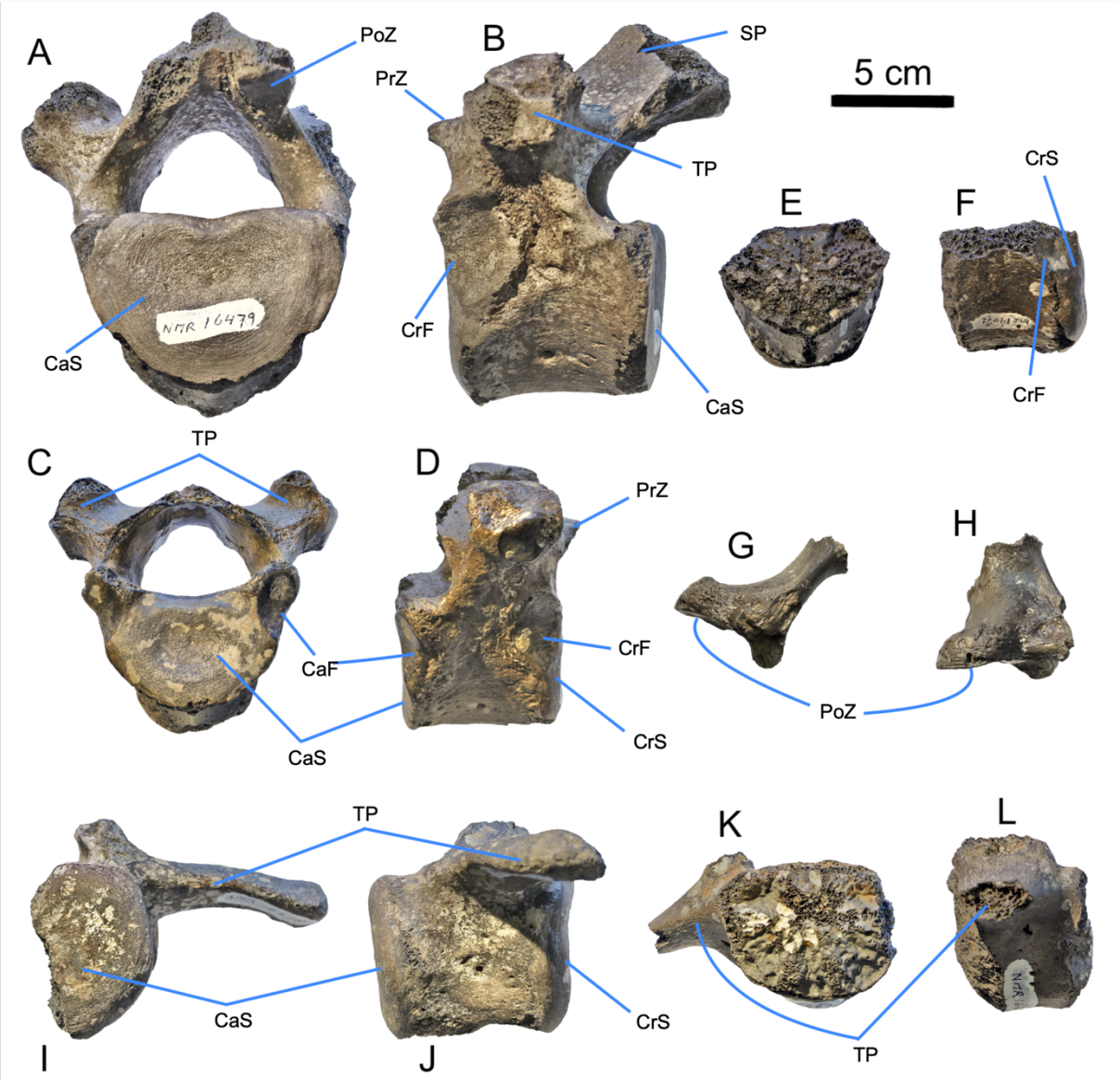

***Figure 18**: A-B caudal and left side view of the 11th thoracic vertebra NMR999100016479; C-F caudal and right side view of respectively a 5th, 6th or 7th thoracic vertebra NMR999100016480 and a 4th or 5th thoracic vertebra NMR999100014072; G-H cranial and right side view of a 6th or 7th cervical vertebra IRSNB-34228-039; I-J caudal and right side view of a lumbar vertebra IRSNB-34228-037; K-L caudal and left side view of a lumbar vertebra IRSNB-34228-057. CrF cranial costal fovea; CaF caudal costal fovea; CrS cranial articular surface; CaS caudal articular surface; PrZ prezygapophysis; PoZ postzygapophysis; SP spinous process; TB transversal process.*

(*processus spinosus)* are broken off. Compared to the other vertebra of a recent adult female walrus from the collection of the IRSNB, it can possibly be assigned as the 5th, 6th or 7th thoracic vertebra. Because of the small width over the transversal processes, it might have belonged to a juvenile specimen. Specimen NMR 999100016479 is the largest of the vertebra that was examined for this study. The right transversal process is broken off and from the right one, the external bone layer is partly eroded so that the materia spongiosa has become visible. The left prezygapophysis is broken in half.

***Table 11**: Measurements in mm of vertebrae (names in bold) compared with the recent female walrus IRSNB 1150B.*

	NMR 9991000 16480	***NMR 9991000 16479***	***IRSNB 34228-057***	***IRSNB 34228-037***	***NMR 9991000 14072***	*IRSNB 1150 B*						
type	thoracic	thoracic	lumbar	lumbar	thoracic	thoracic	thoracic	thoracic	thoracic	lumbar	lumbar	lumbar
nr	th 5/6	th 11	?	L 5?	th 4/5?	th 5	th 6	th 7	th 11	L 3	L 4	L 5
V1 width over the transversal processes	115	> 128	/	± 212	/	144	139	139	123	169	171	176
V2 max. total height	> 97	> 138	/	/	/	149	150	145	112	128	130	137
V3 transversal length over the prezygapophyses	± 42	70	/	/	/	57	55	55	50	65	68	71
V4 transversal length over the postzygapophyses	/	> 61	/	/	/	52	53	52	60	60	63	63
V5 antero-posterior length over the zygapophyses	> 53	112	/	/	/	91	93	93	103	103	101	95
V6 height of the neural canal	41	43	/	/	/	39	40	42	38	32	33	36
V7 max. width of the neural canal	44.5	56	/	/	/	50	51	54	55	51	48	50
V8 basal length of the neural canal	48	76	> 52	69.5	> 54.6	60	62.6	64.6	65	76	73	69

On the caudal side, the left postzygapophysis is eroded together with the largest part of the spinous process. The absence of caudal costal foveae (*foveae costalis caudalis)* and the fact that the postzygapophyses are ventral directed, makes it possible to assign this as the 11th thoracic vertebra. Because of its large size, it was probably an adult male individual.

Specimen IRSNB-34228-037 and IRSNB-34228-057 (fig. 21 I-L) are lumbar vertebrae. Only the right half of IRSNB-34228-037 is still preserved and the dorsal part with the zygapophyses and the spinous process is also lost. Since more or less one half of the vertebra is preserved, the total width over the transversal processes could be estimated. The shape of the transversal process might indicate that it possibly represents the 5th lumbar vertebra. Compared with IRSNB-1150B, its transversal width is large, which might indicate that it might represent an adult male.

From specimen IRSNB-34228-057, it is also only the vertebral body that is preserved. The beginning of the left transversal process is still present, the right one is completely missing. The cranial and caudal articular surfaces are eroded and the materia spongiosa is visible. It has a relatively small size and for that reason it was already identified as a juvenile individual.

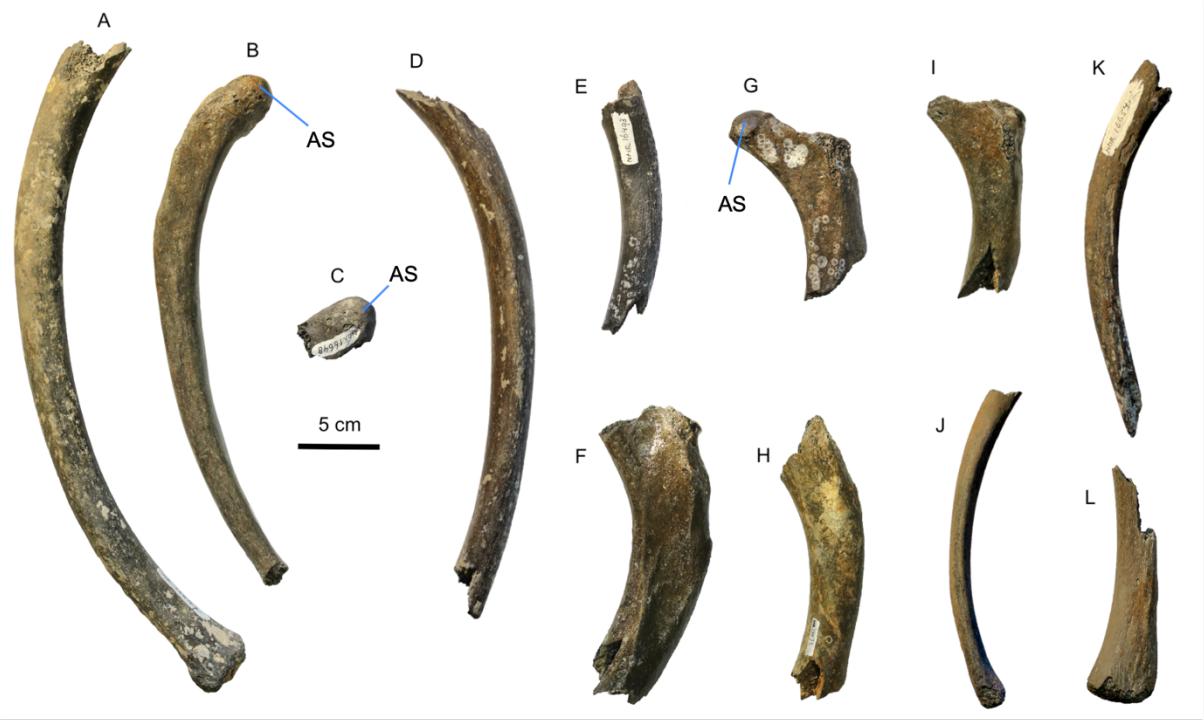

Figure 19: *A-C caudal aspect of left costae respectively with numbers IRSNB-34228-047, NMR 999100016478 & IRSNB-34228-054; D-I cranial aspect of right costae respectively with numbers IRSNB-34228-048, IRSNB-34228-053, NMR 999100014075, IRSNB-34228-052 & NMR 999100014073, NMR 999100014074. J-L undetermined costae respectively with numbers IRSNB-34228-050, IRSNB-34228-055 & IRSNB-34228-058. AS articular surface.*

5.5 Rib

Twelve specimens are (fragments of) ribs (*costae*) (fig.22), but it is very hard to obtain sexual information from this type of bones because there are no noticeable differences. Based on the placement of the articular surfaces on the head and the neck of the ribs and the curvature of the body of the rib, NMR 999100016478, IRSNB-34228-047 & IRSNB-34228-054 could be assigned as left ribs and NMR 999100014073, NMR 999100014074, NMR 999100014075, IRSNB-34228-048, IRSNB-34228-052 & IRSNB-34228-053 as right ribs. For IRSNB-34228-050, IRSNB-34228-055 & IRSNB-34228-058, which represent the lower parts of the ribs, the degree of curvature is not clear enough to assign them to a particular side. Because of its small size, specimen IRSNB-34228-050 has been labelled as a juvenile animal, and the same for specimen IRSNB-34228-047 that was labelled as adult for its large length. For the other specimens, there is no accurate classification possible.

5.6 Humerus

Specimen NMR 999100014071, IRSNB-34228-044 and IRSNB-34228-046 (fig. 23) represent left humeri. Specimens NMR 999100014071 and IRSNB-34228-044 are damaged and only the proximal epiphysis of the bone is preserved. For the former, the proximal epiphysis is completely preserved with the head (*caput)* and the two tubercles. For the latter, on the other hand, only the head and the greater tubercle (*tuberculum majus)* are preserved. The proximal epiphysis of specimen IRSNB-34228-046 has been damaged by abrasion and is broken off. The top part of the crest of the greater tubercle is abraded, but the damaged area decreases in distal direction. The distal epiphysis with the condyle and the capitulum is also not preserved. Measurements of the specimens are shown in table 14. The fact that the epiphyses are either not preserved or found separately from the bone might be an indication that the animals were not yet fully mature and the epiphyses were not yet completely fused to the diaphysis. For the first two specimens, the transverse measurement of the head could be used for comparison with other specimens described by Erdbrink and Van Bree (1986, 1999). Based on this length, I assume that NMR 999100014071 is a subadult male. IRSNB-34228-044 is a more difficult sample to identify because the lesser tubercle (*tuberculum minor)* is almost completely absent, so the transversal length of the caput could not be measured completely, but it is assumed to be from a subadult male. Looking at the measurements of the small diaphysis, IRSNB-34228-046 probably from a juvenile individual. The specimen was already labelled juvenile, which confirms the identification.

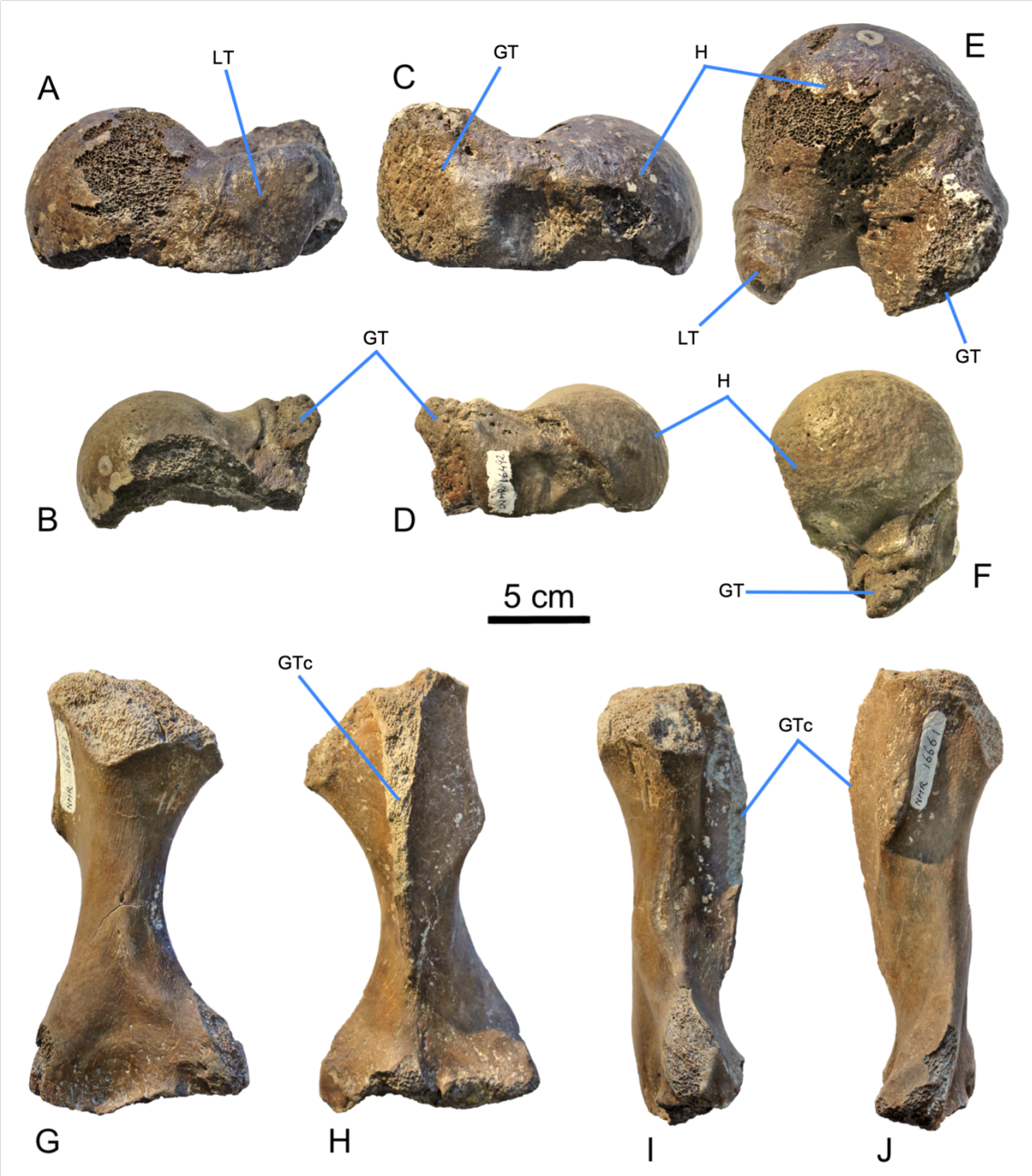

***Figure 20**: A-F lateral, medial and proximal aspects of respectively left humeri NMR 999100014071 and IRSNB-34228-044. G-H caudal, cranial, medial and ventral aspect of left humerus IRSNB 34228-046. LT lesser tubercle; GT greater tubercle; GTc crest of the greater tubercle; H head.*

5.7 Radius

Specimens NMR 999100016764, NMR 999100012537 and IRSNB-34228-045 (fig. 24 A-F) are radii. The proximal epiphysis consisting of the head (*caput radii)* and the distal epiphysis with the styloid process (*processus styloideus)* of all the three specimens are not preserved. This might indicate that

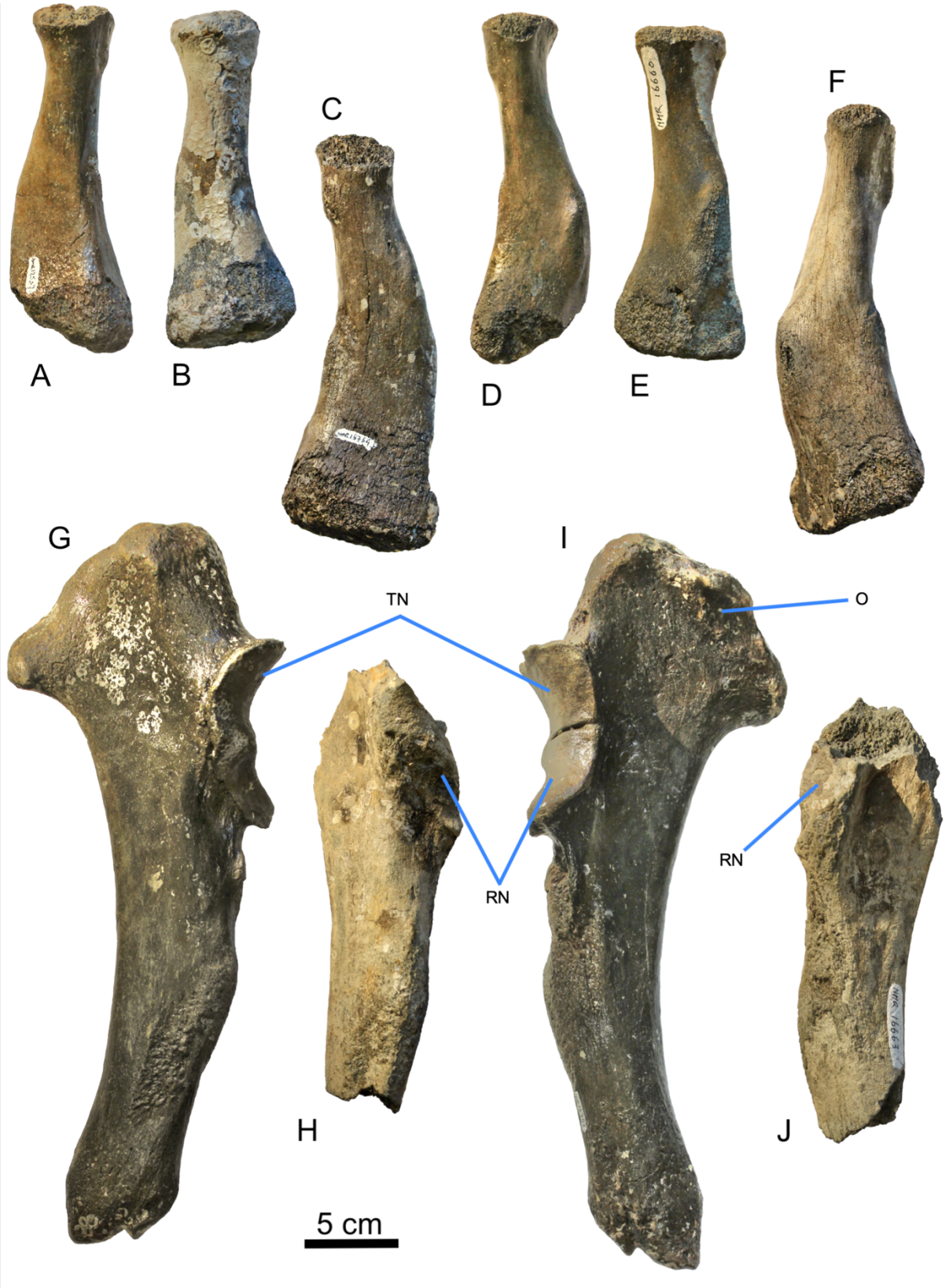

***Figure 21**: A-F respectively medial and lateral aspects of the right radii NMR 999100012537 and IRSNB-34228- the left radius NMR 999100016764. G-J respectively lateral and medial aspects of the right ulnae NMR 999100013792 and IRSNB-34228-051. O olecranon; RN radial notch; TN trochlear notch.*

***Table 12**: Measurements in mm of the humeri (names in bold) compared with humeri described by (Erdbrink and van Bree, 1986, 1999a; Harington and Beard, 1992).*

	NMR 999100014071	***IRSNB 34228-044***	***IRSNB 34228-046***	*N.Z. 53*	*N.Z. (coll. Stolzenbach)*	*ZMA 22.648*	*ZMA 22.649*	*NMC 38490 (L/R)*	*St. 122611*	*St. 170510*	*ZMA 24.613*
Sex (M/F/J)				F	M	M	M	F	F?	F	M
H1 max. length	/	/	> 210	189	378	329	349	343/350	302	312	352
H2 transversal proximal width	123	> 106	> 88	/	116	114	107	102.9	90	86	119
H3 sagittal proximal width	108	89	> 70	/	/	/	/	/	/	/	/
H4 transversal distal width	/	/	± 106	91	144	117	119	/	110	109	137
H5 sagittal distal width	/	/	> 40	/	74	68	73	/	64	63	80
H6 transversal width at the centre of the diaphysis	/	/	38	35	53	/	/	45.2/45.4	41	39	52
H7 sagittal width at the centre of the diaphysis	/	/	37	35	49.6	40	46	37.5/38.5	39	49	45
H8 min. circumference of the diaphysis	/	/	140	152	205	/	/	/	164	158	214

***Table 13**: Measurements in mm of radii (names in bold) compared with specimens described by* (Bisaillon and Piérard, 1981; Erdbrink and van Bree, 1986, 1999b)

	NMR 999100016764	***NMR 999100012537***	***IRSNB 34228-045***	*IRSNB 1150B (L/R)*	*VMUM 75-01-31*	*VMUM 75-02-01*	*ZMA 21.076*	*St. 145446*
Sex (M/F/J)				F	M	F	M	J
R1 length along ulnar side	± 202	177	170	203/224	/	/	295	173
R2 length along posterior side over the crest	> 218	181	176	226/239	281	219	320	82
R3 max. transversal distal width	47	40	40	52/51	/	/	/	> 52
R4 max. sagittal distal width	83	60	67	81/76	/	/	/	
R5 max. proximal width	> 50	46	49	62/63	/	/	/	> 76

They are not fully mature animals. Specimen NMR 999100012537 also lacks part of the trochlea on the caudal side that has been abraded. Both NMR 999100012537 and IRSNB-34228-045 are right radii and have a similar size. The lack of the epiphyses and their relative small size compared to other specimens described by Erdbrink and Van Bree (1986, 1999) and Harington and Beard (1992), might indicate that they are probably juvenile animals. NMR 999100016764 is a left radius and is considerably larger than the other two radii. The specimen shows similar length measurements as the female walrus skeleton IRSNB-1150B from the IRSNB collection and the one described by Bisaillon and Piérard (1981), but the proximal side of the diaphysis is broader. Therefore, and because the specimen is not completely adult, it might possibly be a subadult male. Measurements are shown in table 15.

5.8 Ulna

Specimen NMR 999100013792 and IRSNB-34228-051 (fig. 24 G-J) are two right ulnae, of which NMR 999100013792 is complete and very well-preserved. It shows almost no signs of abrasion. The proximal and distal ends of IRSNB-34228-051 are broken off and only the middle part of the diaphysis is preserved. The bone is broken on the proximal end just above the radial notch (*incisura radialis)*, which is also damaged, and the trochlear notch (*incisura trochlearis*) and the olecranon are gone. On the distal end, the bone is broken off just below the knickpoint of the bone on the cranial side. Measurements of both specimens can be found in table 16. Based on comparison with the specimen described by Bisaillon and Piérard (1981) and Harington and Beard (1992), NMR 999100013792 can be identified as an adult male because of the large size of the bone. Due to the lack of other measurements, IRSNB-34228-051 could only be compared to the adult female walrus described by

***Table 14**: Measurements in mm of ulnae (names in bold) compared with a specimen described by* (Harington and Beard, 1992).

	NMR 999100013792	***IRSNB 34228-051***	*IRSNB 1150 B (L/R)*	*NMC 38490 (L/R)*
Sex (M/F/J)			F	F
R6 max. length of the ulna	377	>>226	313/308	347/348
R7 max. transversal distal width	59	/	47/48	51.7/52.7
R8 max. sagittal distal width	37	/	29/30	34.9/35.8
R9 min. transversal width of the diaphysis	50	± 51	34/33	40/40.2
R10 min. sagittal width of the diaphysis	32	± 32	23/24	23.8/23.9
R11 length over the olecranon	128	/	94/93	84.9/85.8

Harington and Beard (1992) and the female walrus from the IRSNB collection. Looking at the transversal and sagittal width of the diaphysis, which is also similar as in NMR 999100013792, I presume that it is also an adult male.

5.9 Pelvis

The specimens IRSNB-34228-059, NMR 999100012536 and IRSNB-34228-033 (fig. 25 A-E) are all parts of the pelvis. Measurements are displayed in table 17. IRSNB-34228-059 and NMR 999100012536 are both ilium bones, respectively from the right and the left innominate, with approximately half (NMR 999100012536) and two thirds (IRSNB-34228-059) of the acetabulum preserved. The former is the smallest of both fossils and well-preserved, showing only small abrasion marks on the iliac crest. On its medial side, the sacropelvic joint can be clearly distinguished. The acetabulum is quite deep and the iliopubic eminence is not much pronounced. The latter iliopubic eminence is well-developed and the acetabulum has a large diameter but is quite shallow. The rims of the acetabulum and the crest of the ilium are much more rounded than NMR 999100012536, which shows that it suffered more from abrasion. This also caused that the sacropelvic joint, on the medial side of the bone, cannot be very well distinguished. Samples have been taken from the ventral side of the ilium by the VLIZ for DNA-analysis in a still-ongoing study to compare different fossil walrus specimens with modern populations in the North Sea area, but the results were not yet available (pers. comm. Olivier Lambert). Both specimens were compared with the modern female innominate from IRSNB-1150B and with the adult male specimen St. 400978 described by Erdbrink and Van Bree (1999b). The small acetabulum from NMR 999100012536 and the overall size of the bone shows a great resemblance with the female specimen. Therefore, I suggest that it also belonged to an adult female. The larger specimen IRSNB-34228-059 on the other hand, is more similar to the male specimen St. 400978. The only remarkable difference is the circumference of the iliac column, which is with 183 mm almost double than the 103 mm for St. 400978 and the width of the iliac column is three times larger. As Erdbrink and Van Bree state that the bone has little abrasional damage on the place where this is measured, abrasion is not an explanation. It is might be possible that the bone was exceptionally thin. Unfortunately, there was little other material available for further comparison. Despite this difference, I suggest that IRSNB-34228-059 was also an adult male.

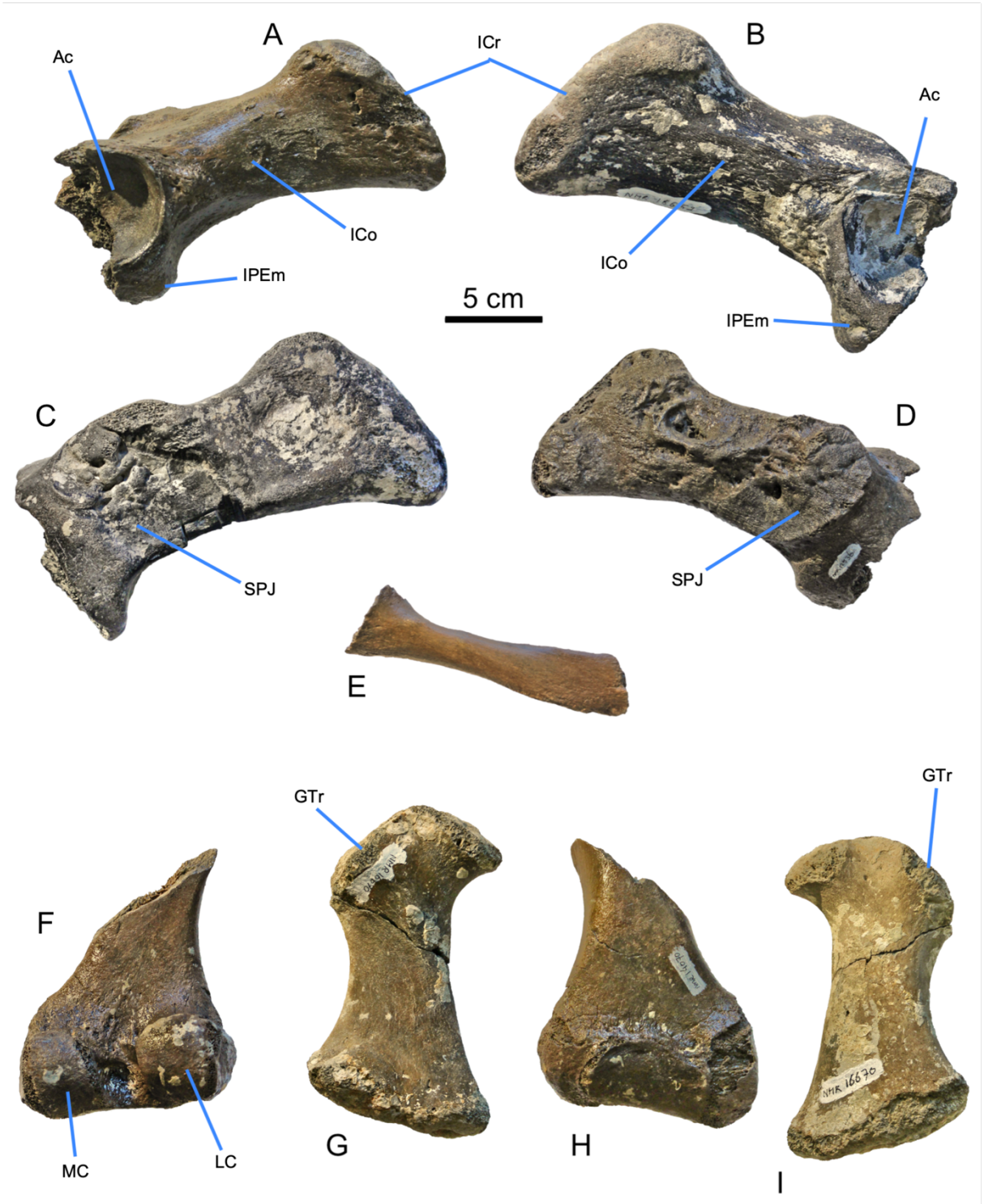

***Figure 22**: A-D respectively lateral and medial aspect of right innominate NMR 999100012536 and left innominate IRSNB 34228-059; E medial aspect of a pubis bone from a left innominate with number IRSNB-34228-033. F-I respectively caudal and cranial aspects of right femur NMR999100014070 and left femur IRSNB-34228-040. Ac acetabulum; ICo iliac column; ICr iliac crest; IPEm iliopubic eminence; SPJ sacropelvic joint; GTr greater trochanter; MC medial condyle; LC lateral condyle.*

***Table 15**: Pelvis measurements (names in bold) in mm compared with specimens described by* (Erdbrink and Van Bree, 1999).

	IRSNB 34228-059	***NMR 999100012536***	*St. 400978*	*IRSNB 1150B (L/R)*
Sex (M/F/J)			M	F
P1 max. length of the ilium	202	179	/	183
P2 max. depth of the acetabulum	> 19	± 26	24	26
P3 diameter of the acetabulum at right angles of the direction of the obturator foramen	± 67	54	64	52/53
P4 min. width of the iliac column	63	55	23	58/57
P5 min. height of the iliac column	46	32	34	34/33
P6 thickness of the bone at the edge of the acetabulum	> 49	57	51	44
P8 width over the iliac crest	± 115	99	/	117/119
P7 min. circumference of the iliac column	183	153	103	157/163

Specimen IRSNB-34228-033 is a fragment of a pubis bone from the left innominate. It is a small and elongated bone, flattened on its caudal side and has a total length of 137 mm. Not much comparable material is available and there are no sexual differences described about the pubis bone, hence it is not very useful for this investigation.

5.10 Femur

NMR 999100014070 and IRSNB-34228-040 (fig. 25 F-I) are femora. Specimen NMR 999100014070 is a right femur where only the distal part of the femur is preserved. The bone is obliquely broken more or less in the narrowest part of the diaphysis and the inner bony materia spongiosa is sticking out of the middle of the bone. Both condyles are well-developed with the lateral condyle slightly larger than the medial condyle. Specimen IRSNB-34228-040 represents a left femur and is broken in two pieces, but they can still be put together for measurement. The fracture runs obliquely from the lower end of the greater trochanter (*trochanter major)* to a bit above the middle of the diaphysis. Both proximal and distal epiphyses are not preserved. There are also no signs of the lesser trochanter (*trochanter minor*) or the intertrochanteric crest. Table 18 displays some measurements of the bones. Because of the small size of the bone and absence of the epiphyses, IRSNB-34228-040 probably represents a juvenile animal. NMR 999100014070 is compared with femora of the recent walrus IRSNB-1150 B from the collection of the IRSNB and with other fossil femora described by Erdbrink and Van Bree (1999). When looking at

the measurements of the transversal and sagittal width over the condyles, it shows the greatest resemblance with femora from adult females.

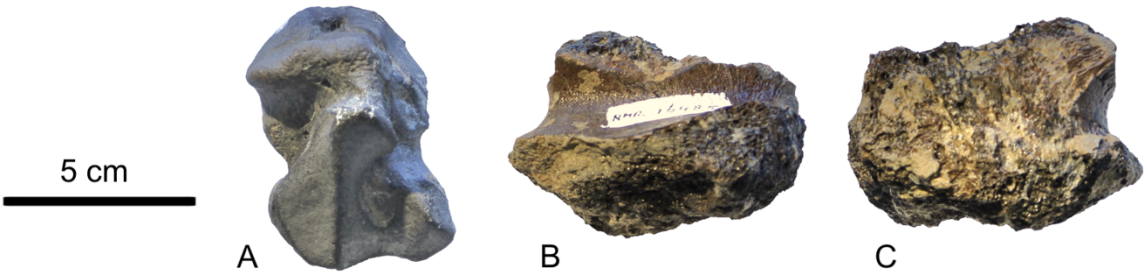

***Figure 23**: A posterior view of the right cuboid bone IRSNB-34228-038. B-C different aspects of an indeterminate fragment IRSNB-34228-056.*

5.11 Tarsal

Specimen IRSNB-34228-038 (fig. 26 A) is a right cuboid bone, which is relatively well-preserved and the fourth of the seven tarsal bones in the hind flipper of the walrus. With a maximal width of 46 mm and total length of 69 mm, the bone seems to have a significant larger size than the female IRSNB-1150B, which has a width of 38 mm and total length of 63 mm. Therefore, it might be possible that it belonged to an adult male walrus. However, there is little comparative material is for this bone and it was not possible to compare the specimen with tarsal bones from a male individual.

Specimen IRSNB-34228-056 (fig. 26 B-C) is the last bone fragment that was available for this study, but it is in a poor condition and could not be identified.

***Table 16**: Measurements in mm of femora (names in bold) compared with specimens described by* (Erdbrink and van Bree, 1999b).

	NMR 999100014070	***IRSNB 34228-040***	*IRSNB 1150B*	*KP 472*	*KP 826*	*ZMA 23.396*	*ZMA 23.395*	*St. 147067*
Sex (M/F/J)			F	M	F	M?	F?	M
F1 max. length over the greater trochanter	/	± 153	194	235	163	219	172	210
F2 max. proximal width (head-greater troch.)	/	> 87	111	136	91	116	95	100
F3 transversal min. width over the centre of the diaphysis	± 54	50	55	65.5	51	62	52	58
F4 sagittal min. width over the centre of the diaphysis	27	26	22	48	29	35	27	37.5
F5 transversal width over the condyles	108	93	105	129	± 98	116	97	117

F6 sagittal width over the condyles	55	/	51	70	± 50	59	51	59
F7 circumference at the centre of the diaphysis	± 140	131	141	173	142	154	140	156

6 DISCUSSION

Of the walrus fossils that were found in *Het Scheur*, 43 were available for this study, of which 29 (about two third of the specimens) could be used to give information about possible walrus colonies. The other specimens (mostly ribs) do not show enough sexual differences to do an accurate identification of the sex of the bone. Sex could be assigned to 20 specimens. Nine others could be identified as juvenile individuals due to their small size and the lack of fusion between the epiphysis and diaphysis. Differences in sexual size dimorphism are not yet expressed in young walruses, which makes it impossible to make an accurate identification of the sex of young individuals. For some bone types, such as the cuboid bone or the vertebra, the identification of the sex is not very certain, because only little comparable material from fossils or recent walruses for these parts has been described in the literature. Of the 20 of which the sex could be identified specimens, six could be identified as subadult males, ten as adult males and four as adult females. Subadult males are counted together with adult males as they already left their mothers and have joined all-male herds. If the relation of females + juvenile to males is plotted (fig. 27), a ratio of 45% to 55% is obtained.

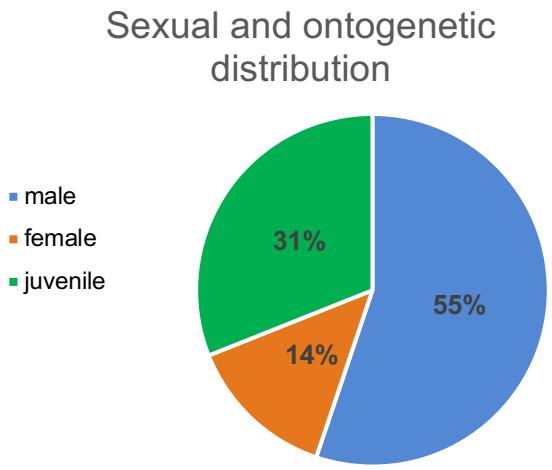

***Figure 24**: Sexual and ontogenetic distribution of the fossil remains at Het Scheur.*

Mixed colonies of males, females and juveniles occur only during the breeding season, but generally consist only for up to 10 % of males (Fay, 1982), and therefore seems highly unlikely as an explanation for the makeup of this fossil record. Because the two groups live in separate herds for the larger part of the year, it would be expected that one or the other group is dominant if the location was only inhabited by one group over time. However, the percentage of males for these fossils is only slightly higher than the combined percentage of females and juveniles.

It is possible that mixed walrus colonies occurred in the Nord Sea Basin during the Pleistocene, but no investigation has been done yet on the sexual composition of Pleistocene walrus colonies as large. Looking at the ratio between (sub-)adult males and (sub-)adult females, the scenario of a mixed colony seems rather unlikely. As recent research on modern walruses has shown that the mortality of adult males is just slightly higher than for females (Born et al., 1995; Fay, 1982), it would be rather unlikely that in a healthy group the mortality of (sub-)adult males would have been almost four times as high as for (sub-)adult females. The high number of juvenile fossils compared to (sub-)adult females, could possibly be a reflection of a higher mortality among young animals (Born et al., 1995; Fay, 1982).

A more plausible hypothesis for this distribution between both male and female (sub-)adults and juveniles could be that the location was used as a haul-out site by several walrus colonies. This could be two colonies that were hauled-out close to this location or, more likely, different colonies that occupied the site during different timespans. I propose two possible situations: 1) a shift from the occupation of the site by all-male herds to female-juvenile herds or vice-versa or 2) an occupation of the site by walrus colonies that regularly (annually to semi-annually) alternated between all-male herds and female-juvenile herds. The change of colonies could be the result of the annual walrus migration following the sea ice border (Born et al., 1995; Fay, 1982) As female walruses tend to be more migratory, it could imply that during winter a female-juvenile herds was hauled-out at the site, which migrated north during summer with the sea ice border and an all-male herd would take its place. The large number of fossils may indicate that the location was a regularly visited haul-out site.

De Clercq (2018) suggests a Late Eemian to Early Glacial origin of these *Odobenus* fossils, based on the paleogeographic reconstructions of the BCS. A probable relation to the walrus tusk found on the beach near Ostend in 2014 (fig. 28), was suggested based on stratigraphic analysis. This may indicate that the walrus occurrence on the BCS was not only limited to *Het Scheur* at the end of the Eemian and the beginning of the Last Glacial. As there are also large numbers of well-preserved walrus fossils

collected East of *Het Scheur* in the Wielingen channel, which is about 10-20 km from the study area and comprises an area of about 50 km^2, it might be possible that there were also haul-out locations in that area. Most of these fossils are currently in the collection of the NMR and not investigated for this study. Unfortunately, the exact locations of these fossils are lacking, as most of them were collected during fishing activities. Further paleogeographic reconstructions for the same period for the Dutch part of the Wielingen could show more possible haul-out locations for walrus colonies at the end of the Eemian and the beginning of the Last Glacial (fig. 28).

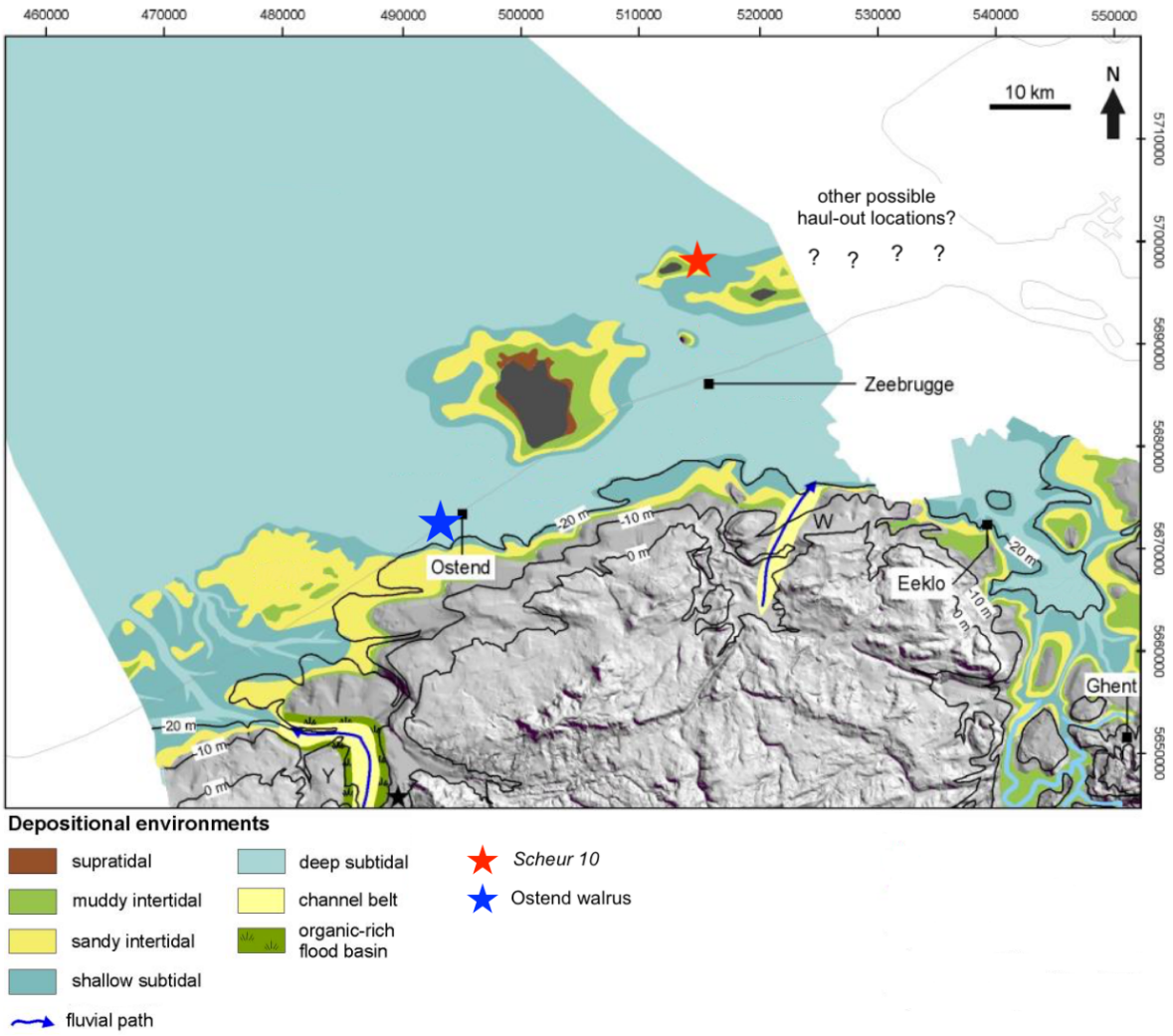

***Figure 25**: Paleogeographic reconstruction of the Late Eemian/Early Glacial landscape of the BCS with indications of walrus finds. Modified after De Clercq (2018).*

7 CONCLUSION

Of the 43 *Odobenus rosmarus* fossils that were investigated for this study, about two third could give some information about the sexual and ontogenetic makeup of the walrus colony. Considering similar sexual size dimorphism as seen in modern walruses, those 29 fossils were be identified as juveniles (9), (sub-)adult males (16) and (sub-)adult females (4), showing only a small majority (55 %) of the male animals compared to the combined juveniles and female animals (45 %). Looking at the large percentage of male animals and the fact that modern *Odobenus* live in sexually segregated herds most of the time, a mixed colony seems rather unlikely. A more acceptable hypothesis suggests that the walrus occupancy at *Het Scheur* alternated between all-males herds and females-juvenile herds. This could either be regular alternations on an (semi-)annually timescale or just a single shift from one type of colony to another. The change in colony may be the result of the migratory behaviour of the walrus. Despite the ambiguous radiocarbon ages of 44-50 ka, recent paleogeographic reconstructions of the BCS propose a Late Eemian to Early Glacial origin for the fossils. Together with other walrus finds from Ostend and the Wielingen channel, this may suggest a larger occupancy of the BCS than only at *Het Scheur* during the Middle-Late Eemian and Early Glacial.

Further planned dating of shell residue fished up together with the fossils and investigation of paleoclimate indicators (pollen, diatoms, dinoflagellates) can yield more information about the age of the fossils and the climate of the site during the occupation of the walrus colonies, but this is outside the scope of this project. The acquisition of shallow sediment cores near the site in combination with the obtained seismic data, would make it possible to make a more detailed paleogeographic reconstruction of the study area. Investigation of other fossil walrus specimens from the nearby Wielingen channel might possibly also give additional information about the presence of walruses on the BCS during the Middle-Late Eemian and the beginning of the Last Glacial.

8 BIBLIOGRAPHY

Allen, J.A., 1880. History of North American Pinnipeds, a monograph of the walruses, sea-lions, sea-bears and seals of North America. U.S. Geological and Geographical Survey of the Territories, Miscellaneous publications 12, xvi + 765. https://doi.org/10.5962/bhl.title.23136

Barnes, L.G., 1988. A new fossil pinniped (Mammalia: Otariidae) from the middle Miocene Sharktooth Hill bonebed, California. Contributions in Science 396, 1–11.

Barnes, L.G., Raschke, R.E., 1991. Gomphotaria Pugnax, a new genus and species of late Miocene Dusignathine Otariid Pinniped (Mammalia: Carnivora) from California. Contributions in Science 426, 1–16.

Berta, A., 2018. Pinniped Evolution, in: Würsig, B., Thewissen, J.G.M., Kovacs, K.M. (Eds.), Encyclopedia of Marine Mammals. Elsevier, pp. 712–722. https://doi.org/10.1016/B978-0-12-804327-1.00196-5

Berta, A., Churchill, M., Boessenecker, R.W., 2018. The Origin and Evolutionary Biology of Pinnipeds: Seals, Sea Lions, and Walruses. Annual Review of Earth and Planetary Sciences 46, 203–228. https://doi.org/10.1146/annurev-earth-082517-010009

Bisaillon, P.A., Piérard, J., 1981. Ostéologie du Morse de l'Atlantique (Odobenus rosmarus, L., 1758) Ceintures et members. Anatomia, Histologia, Embryologia 10, 310–327. https://doi.org/10.1111/j.1439-0264.1981.tb00696.x

Boessenecker, R.W., Churchill, M., 2013. A Reevaluation of the Morphology, Paleoecology, and Phylogenetic Relationships of the Enigmatic Walrus Pelagiarctos. PLoS ONE 8, e54311. https://doi.org/10.1371/journal.pone.0054311

Born, E.W., Gjertz, I., Reeves, R.R., 1995. Population Assessment of Atlantic walrus (Odobenus rosmarus rosmarus L.).

Bot, S. Le, Lancker, V. Van, Deleu, S., Batist, M. De, Henriet, J.P., 2003. Tertiary and Quaternary Geology of the Belgian Continental Shelf. Science Policy Office, Brussels, Belgium.

Caspers, G., Freund, H., 2001. Vegetation and climate in the Early- and Pleni-Weichselian in northern Central Europe. Journal of Quaternary Science 16, 31–48. https://doi.org/10.1002/1099-1417(200101)16:1<31::AID-JQS577>3.0.CO;2-3

Chapskii, K.K., 1940. Distribution of walrus in the Laptev and East Siberian Seas. Problemy Arktiki 6,

80–84.

Cohen, K.M., MacDonald, K., Joordens, J.C.A., Roebroeks, W., Gibbard, P.L., 2012. The earliest occupation of north-west Europe: A coastal perspective. Quaternary International 271, 70–83. https://doi.org/10.1016/j.quaint.2011.11.003

Cohen, K.M., Westley, K., Erkens, G., Hijma, M.P., Weerts, H.J.T., 2017. Submerged Landscapes of the European Continental Shelf, Submerged Landscapes ofthe European Continental Shelf: Quaternary Paleoenvironments. Wiley. https://doi.org/10.1002/9781118927823

Commitee on Marine Mammals, (1966-1967), 1967. Standard Measurements of Seals. Journal of Mammalogy 48, 459. https://doi.org/10.2307/1377778

Cronin, M.A., Hills, S., Born, E.W., Patton, J.C., 1994. Mitochondrial DNA variation in Atlantic and Pacific walruses. Canadian Journal of Zoology 72, 1035–1043. https://doi.org/10.1139/z94-140

Cullen, T.M., Fraser, D., Rybczynski, N., Schröder-Adams, C., 2014. Early evolution of sexual dimorphism and polygyny in Pinnipedia. Evolution 68, 1469–1484. https://doi.org/10.1111/evo.12360

Davies, J.L., 1958. Pleistocene Geography and the Distribution of Northern Pinnipeds. Ecology 39, 97. https://doi.org/10.2307/1929971

De Clercq, M., 2018. Drowned landscapes of the Belgian Continental Shelf: implications for northwest European landscape evolution and preservation potential for submerged heritage. Ghent University, Belgium.

De Clercq, M., Missiaen, T., Wallinga, J., Zurita Hurtado, O., Versendaal, A., Mathys, M., De Batist, M., 2018. A well-preserved Eemian incised-valley fill in the southern North Sea Basin, Belgian Continental Shelf - Coastal Plain: Implications for northwest European landscape evolution. Earth Surface Processes and Landforms 43, 1913–1942. https://doi.org/10.1002/esp.4365

Deméré, T.A., 1994. Two new species of fossil walruses (Pinnipedia:Odobenidae) from the Upper Pliocene San Diego Formation, California. Proceedings of the San Diego Society of Natural History 29, 77–98.

Deméré, T.A., Berta, A., 2001. A reevaluation of proneotherium repenningi from the miocene astoria formation of oregon and its position as a basal odobenid (pinnipedia: Mammalia). Journal of Vertebrate Paleontology 21, 279–310. https://doi.org/https://doi.org/10.1671/0272-4634(2001)021[0279:AROPRF]2.0.CO;2

Deméré, T.A., Berta, A., 1994. The family Odobenidae: a phylogenetic analysis of living and fossil forms. Proceedings of the San Diego Society of Natural History 29, 99–123.

Du Four, I., Schelfaut, K., Vanheteren, S., Van Dijk, T., Van Lancker, V., 2006. Geologie en sedimentologie van het westerscheldemondingsgebied, in: Coosen, J., Mees, J., Seys, J., Fockedey, N. (Eds.), Studiedag: De Vlakte van de Raan van Onder Het Stof Gehaald. Oostende, 13 Oktober 2006. VLIZ Special Publication 35, pp. 16–29.

Dutton, A., Lambeck, K., 2012. Ice Volume and Sea Level During the Last Interglacial. Science 337, 216–219. https://doi.org/10.1126/science.1205749

Erdbrink, B., van Bree, P.J.H., 1986. Fossil Odobenidae in some dutch collections (Mammalia, Carnivora). Beaufortia 36, 13–33.

Erdbrink, D.P.B., van Bree, P.J.H., 1999a. Fossil cranial walrus material from the North Sea and the estuary of theSchelde (Mammalia, Carnivora). Beaufortia 49, 1–9.

Erdbrink, D.P.B., van Bree, P.J.H., 1999b. Fossil appendicular skeletal walrus material from the North Sea and the estuary of the Schelde (Mammalia, Carnivora). Beaufortia 49, 63–81.

Erdbrink, D.P.B., Van Bree, P.J.H., 1999. Fossil axial skeletal walrus material from the North Sea and the estuary of the Schelde, and a fossil sirenian rib (mammalia, carnivora; sirenia). Beaufortia 49, 11–20.

Fay, F.H., 1982. Ecology and Biology of the Pacific Walrus, Odobenus rosmarus divergens Illiger. North American Fauna 74, 1–279. https://doi.org/10.3996/nafa.74.0001

Fay, F.H., Carleton Ray, G., Kibal'chich, A.A., 1984. Time and location of mating and associated behavior of the Pacific Walrus, Odobenus rosmarus divergens Illiger. Soviet-American cooperative research on marine mammais 1, 89–99.

Garlich-Miller, J.L., Stewart, R.E.A., 1998. Growth and sexual dimorphism of Atlantic walruses (Odobenus rosmarus rosmarus) in Fox Basin, Northwest Territories, Canada. Marine Mammal Science 14, 803–818. https://doi.org/10.1111/j.1748-7692.1998.tb00764.x

Gingras, M.K., Armitage, I.A., Pemberton, S.G., Clifton, H.E., 2007. Pleistocene walrus herds in the Olympic Peninsula area: trace-fossil evidence of predation by hydraulic jetting. Palaois 22, 539–545.

Hablützel, P., Langeveld, B., De Clercq, M., Post, K., Mol, D., Vandorpe, T., De Rijcke, M., Lambert, O., Missiaen, T., Vandegehuchte, M.B., 2018. The walrus (Odobenus rosmarus): a distinctive member

of the Pleistocene megafauna in Belgium, in: Mees, J.; Seys, J. (Ed.), Book of Abstracts – 53rd European Marine Biology Symposium. Vlaams Instituut voor de Zee - Flanders Marine Institute (VLIZ), Oostende, Belgium, p. 46.

Harington, C.R., 1984. Quaternary marine and land mammals and their paleoenvironmental implications - some examples from northern North America. Carnegie Museum of Natural History Special Publications 8, 511–525.

Harington, C.R., 1975. A postglacial walrus (Odobenus rosmarus) from Bathurst Island, Northwest Territories. The Canadian Field-Naturalist 89, 249–261.

Harington, C.R., Beard, G., 1992. The Qualicum walrus: a late Pleistocene walrus (Odobenus rosmarus) skeleton from Vancouver Island, British Columbia, Canada. Annales Zoologici Fennici 28, 311–319.

Helmens, K.F., 2014. The last interglacial-glacial cycle (MIS 5-2) re-examined based on long proxy records from central and northern europe. Quaternary Science Reviews 86, 115–143. https://doi.org/10.1016/j.quascirev.2013.12.012

Hocking, D.P., Marx, F.G., Wang, S., Burton, D., Thompson, M., Park, T., Burville, B., Richards, H.L., Sattler, R., Robbins, J., Miguez, R.P., Fitzgerald, E.M.G., Slip, D.J., Evans, A.R., 2021. Convergent evolution of forelimb-propelled swimming in seals. Current Biology 31, 2404-2409.e2. https://doi.org/10.1016/j.cub.2021.03.019

Horikawa, H., 1994. A primitive odobenine walrus of Early Pliocene age from Japan. The Island Arc 3, 309–328. https://doi.org/10.1111/j.1440-1738.1994.tb00118.x

Kardas, S.J., 1965. Notas sobre el genero Odobenus (Mammalia, Pinnipedia). 1. Una nueva suespecie fosil del Pleistoceno superior-Holoceno. Bol. B. Soc. Espanola Hist. Nat.(Biol.) 63, 363–380.

Kastelein, R. a, Gerrits., N.M., 1990. The anatomy of the walrus head (Odobenus rosmarus). Part 1: The skull. Aquatic Mammals 16, 101–119.

Kastelein, R.A., 2002. Walrus, in: Perrin, W.F., Würsig, B., Thewissen, J.G.M. (Eds.), Encyclopedia of Marine Mammals (First Edition). Academic Press, pp. 1294–1300.

Kellogg, R., 1922. Pinnipeds from Miocene and Pleistocene Deposits of California. Bulletin of the Department of Geological Sciences 13, 23–132.

King, J.E., 1964. Seals of the world. The British Museum (Natural History), London, p. 177.

Knutsen, L.Ø., Born, E.W., 1994. Body growth in Atlantic walruses (Odobenus rosmarus rosmarus)

from Greenland. Journal of Zoology 234, 371–385. https://doi.org/10.1111/j.1469-7998.1994.tb04854.x

Kohno, N., 2006. A New Miocene Odobenid (Mammalia : Carnivora) from Hokkaido , Japan , and Its Implications for Odobenid Phylogeny Author (s): Naoki Kohno Reviewed work (s): Published by : Taylor & Francis , Ltd . on behalf of The Society of Vertebrate Paleontology 26, 411–421.

Kohno, N., 1994. A new Miocene pinniped in the genus Prototaria (Carnivora: Odobenidae) from the Moniwa Formation, Miyagi, Japan. Journal of Vertebrate Paleontology 14, 414–426. https://doi.org/10.1080/02724634.1994.10011568

Kohno, N., Ray, C.E., 2008. Pliocene walruses from the Yorktown Formation of Virginia and North Carolina, and a systematic revision of the North Atlantic Pliocene walruses. Virginia Museum of Natural History Special Publication 14, 39–80.

Kohno, N., Tomida, Y., Hasegawa, Y., Furusawa, H., 1995. Pliocene tusked odobenids (Mammalia: Carnivora) in the Western North Pacific, and their paleobiogeography. Bulletin-National Science Museum Tokyo Series C 21, 111–131.

Kopp, R.E., Simons, F.J., Mitrovica, J.X., Maloof, A.C., Oppenheimer, M., 2009. Probabilistic assessment of sea level during the last interglacial stage. Nature 462, 863–867. https://doi.org/10.1038/nature08686

Kovacs, K.M., Lavigne, D.M., 1992. Maternal investment in otariid seals and walruses. Canadian Journal of Zoology 70, 1953–1964. https://doi.org/10.1139/z92-265

Kryukova, N. V., 2012. Dentition in Pacific walrus (Odobenus rosmarus divergens) calves of the year. Biology Bulletin 39, 618–626. https://doi.org/10.1134/S1062359012070072

Laidre, K.L., Stern, H., Kovacs, K.M., Lowry, L., Moore, S.E., Regehr, E. V., Ferguson, S.H., Wiig, Ø., Boveng, P., Angliss, R.P., Born, E.W., Litovka, D., Quakenbush, L., Lydersen, C., Vongraven, D., Ugarte, F., 2015. Arctic marine mammal population status, sea ice habitat loss, and conservation recommendations for the 21st century. Conservation Biology 29, 724–737. https://doi.org/10.1111/cobi.12474

Lambeck, K., Purcell, A., Dutton, A., 2012. The anatomy of interglacial sea levels: The relationship between sea levels and ice volumes during the Last Interglacial. Earth and Planetary Science Letters 315–316, 4–11. https://doi.org/10.1016/j.epsl.2011.08.026

Langeveld, B., 2018. Walrusexpeditie op de Belgische Noordzee. Straatgras 30, 13–15.

Lindenfors, P., Tullberg, B., Biuw, M., 2002. Phylogenetic analyses of sexual selection and sexual size dimorphism in pinnipeds. Behavioral Ecology and Sociobiology 52, 188–193. https://doi.org/10.1007/s00265-002-0507-x

Lindqvist, C., Bachmann, L., Andersen, L.W., Born, E.W., Arnason, U., Kovacs, K.M., Lydersen, C., Abramov, A. V., Wiig, Ø., 2009. The Laptev Sea walrus Odobenus rosmarus laptevi : an enigma revisited. Zoologica Scripta 38, 113–127. https://doi.org/10.1111/j.1463-6409.2008.00364.x

Long, A.J., Barlow, N.L.M., Busschers, F.S., Cohen, K.M., Gehrels, W.R., Wake, L.M., 2015. Near-field sea-level variability in northwest Europe and ice sheet stability during the last interglacial. Quaternary Science Reviews 126, 26–40. https://doi.org/10.1016/j.quascirev.2015.08.021

Lydersen, C., 2018. Walrus, in: Würsig, B., Thewissen, J.G.M., Kovacs, K.M. (Eds.), Encyclopedia of Marine Mammals (Third Edition). Academic press, pp. 1045–1048. https://doi.org/10.1016/B978-0-12-804327-1.00020-0

Medina-Elizalde, M., 2013. A global compilation of coral sea-level benchmarks: Implications and new challenges. Earth and Planetary Science Letters 362, 310–318. https://doi.org/10.1016/j.epsl.2012.12.001

Miller, E.H., 1975. Walrus ethology. I. The social role of tusks and applications of multidimensional scaling. Canadian Journal of Zoology 53, 590–613. https://doi.org/10.1139/z75-073

Missiaen, T., Hablützel, P., De Rijcke, M., Lambert, O., Germonpre, M., Langeveld, B., 2019. The Scheur: A unique prehistoric fossil graveyard off the Belgian coast, in: Mees, J., Seys, J. (Eds.), Book of Abstracts - VLIZ Marine Science Day. Bredene, Belgium. aams Instituut voor de Zee – Flanders Marine Institute (VLIZ), Oostende, Belgium, p. 124.

Mitchell, E.D., 1961. A new walrus from the Imperial Pliocene of southern California: with notes on odobenid and otariid humeri. Contributions in Science 44, 1–28.

Mohr, E., 1942. Geschlechtsunterschiede am Walroß-Schädel. Zoologischer Anzeiger 137, 71–76.

Piérard, J., Bisaillon, A., 1983. Ostéologie du morse de l'atlantique (Odobenus rosmarus, L., 1758). Anatomia, Histologia, Embryologia 12, 33–52. https://doi.org/10.1111/j.1439-0264.1983.tb01000.x

Post, K., 2004. What's in a name - Alachtherium crestii, de Pliocene walrus van de Noordzee. Grondboor & Hamer 3/4, 70–74.

Post, K., 1999. Laat-Pleistocene zeezoogdieren van de Nederlandse kustwateren. Grondboor & Hamer 6, 126–130.

Post, K., Hoekman, A., De Wilde, B., 2017. Oerwalvissen op de bodem van de Noordzee. Cranium 34, 48–51.

Repenning, C.A., Tedford, R.H., 1977. Otarioid Seals of the Neogene. Geological Survey Professional Paper 992 93.

Sanders, A.E., 2002. Additions to the Pleistocene Mammal Faunas of South Carolina, North Carolina, and Georgia. American Philosophical Society, Philadelphia.

Seys, J., 2017. Uniek fossielenkerkhof ontdekt voor Belgische kust. Afzettingen WTKG 38, 54–56.

Taylor, N., Clark, C.T., Misarti, N., Horstmann, L., 2020. Determining sex of adult Pacific walruses from mandible measurements. Journal of Mammalogy 101, 941–950. https://doi.org/10.1093/jmammal/gyaa051

Tomida, Y., 1989. A New Walrus (Carnivora, Odobenidae) from the Middle Pleistocene ofthe Boso Peninsula, Japan, and its Implication on Odobenid Paleobiogeography. Bulletin of the National Science Museum 15, 109–119.

Vermeersch, J., Demerre, I., Pieters, M., Van Haelst, S., De Hauwere, N., 2015. Paleontologische resten afkomstig uit het Belgische deel van de Noordzee of aangetroffen op de aanpalende stranden. Unpublished report SeArch-project WP.

VRT NWS, 2018. Spectaculaire fossielen van walrussen en prehistorische monsterhaai gevonden voor de kust. https://doi.org/https://www.vrt.be/vrtnws/nl/2018/01/12/spectaculaire-fossielen-van-walrussen-en-prehistorische-monsterh/

Wiig, Ø., Born, E.W., Gjertz, I., Lydersen, C., Stewart, R.E.A., 2007. Historical sex-specific distribution of Atlantic walrus (Odobenus rosmarus rosmarus) in Svalbard assessed by mandible measurements. Polar Biology 31, 69–75. https://doi.org/10.1007/s00300-007-0334-7

APPENDIX

***Table I**: Measurements made by Mohr (1942) on 22 walrus skulls from the collection of the Zoologisches Museum Hamburg (ZMH).*

				Skull measurements in mm				*Distance of the upper margins of the tusk alveoli in mm*		*Distance of the upper margins of the tusk alveoli in %*	
lauf nr	Museum number	M/F	known age	length	largest width	rostral width	rostral width in skull length in %	extern	intern	M	F
1	ZMH 48144	M	/	380	300	220	57.9	210	110	28.9	/
2	ZMH 48149	F	/	370	320	205	55.4	205	75	/	20.3
3	ZMH 47658	M	/	375	280	240	64.0	220	100	26.7	
4	ZMH 47970	M	17 yrs	355	240	185	52.1	/	/	/	/
5	ZMH 48145	(M)	/	350	265	165	47.1	170	100	28.6	
6	ZMH 48146	F	/	340	245	150	44.1	145	72	/	21.2
7	ZMH 8571	(F)	/	345	245	150	43.5	160	75	/	21.7
8	ZMH 47657	M	/	315	235	135	42.8	130	80	25.4	/
9	ZMH 48148	F	/	305	215	115	37.7	120	67	/	21.2
10	ZMH 39935	F	7 yrs	290	190	115	39.7	120	60	/	20.7
11	ZMH 48147	(F)	/	300	225	125	41.7	120	65	/	21.7
12	ZMH 47911	F	13 yrs	315	250	115	36.5	120	61	/	19
13	ZMH 41911	F	19 months	255	180	95	37.3	90	46	/	18
14	ZMH 47851	M	17 months	250	170	90	36.0	87	46	18.4	/
15	ZMH 41778	F	14 months	225	160	78	34.7	74	42	/	18.7
16	ZMH 41530	M	16 months	220	170	85	38.6	72	42	19.1	/
17	ZMH 42325	M	8 months	205	160	80	39.0	72	39	19	/
18	ZMH 42310	F	7 months	200	155	76	38.0	68	39	/	19.5
19	ZMH 42648	M	8 months	210	160	75	35.7	70	42	20	/
20	ZMH 47635	M	7 months	/	145	85	/	67	42	/	/
21	ZMH 42232	F	12 months	205	145	75	36.6	73	38	/	18.5